DECAY OF WOODY RESIDUES AS THE COUNTERFACTUAL TREATMENT TO MOBILIZATION FOR BIOELECTRICITY GENERATION

By

Max Arlen Blasdel

A Thesis Presented to

The Faculty of Humboldt State University

In Partial Fulfillment of the Requirements for the Degree

Master of Science in Natural Resources: Environmental and Natural Resource Sciences

Committee Membership

Dr. Kevin Fingerman, Committee Chair

Dr. Jeffrey Kane, Committee Member

Dr. Harold Zald, Committee Member

Dr. Erin Kelly, Graduate Coordinator

July 2020

ABSTRACT

DECAY OF WOODY RESIDUES AS THE COUNTERFACTUAL TREATMENT TO BIOMASS ELECTRICITY MOBILZATION

Max Arlen Blasdel

Decay of woody debris is a major carbon flux for forests. Decay processes are not well documented in forest modeling frameworks but play an important role in forest carbon cycling and life cycle assessments of forest-derived products. The main drivers of decay are species, vertical location, and climate. A database of literature values for decay by tree species was created to parameterize a larger model of California forestland carbon cycling. A novel methodology was applied to vary these decay values for each species spatially based on climatic drivers of decay. This resulted in decay values for each species and size class as well as the weighted average at each site across the state of California. These decay values can be reported as 50% residence times ranging from 4 to 144 years for coarse woody debris, giving forest managers a better sense of how long residues will persist in the field once they are created. The residence times can be further adapted to account for the effect of piling materials on decay rate. This approach could be extended beyond California to show decay variation in other systems.

ACKNOWLEDGEMENTS

I would like to thank the Schatz Energy Research Center for providing a position that allowed me to do this research. This work was part of the California Biomass Impacts Project, which was funded by the California Energy Commission under award number EPC-16-047.

TABLE OF CONTENTS

LIST OF TABLES

LIST OF FIGURES

LIST OF APPENDICES

INTRODUCTION

There is current interest in the use of biomass as a renewable source of electricity as it has the potential to reduce overall greenhouse gas (GHG) emissions, while providing base load renewable energy (EPA, 2014a). One source for biomass fuel is forest residues, which are treated as a waste product in traditional forestry. However, there are also detrimental effects to utilizing biomass, which releases carbon into the atmosphere and produces at least a short-term increase in climate forcing (Giuntoli et al., 2015). Many potential benefits of biomass energy depend on the source of the fuel, harvest circumstances, and eventual fate of the residues (Pierobon et al., 2014).

Residues, or “slash,” remaining after forest harvest or thinning activities are either placed in piles or scattered throughout the forest floor. Residues are often burned as a form of forest management to reduce the threat of forest fires or prepare land for replanting, immediately releasing their stored carbon into the atmosphere (Hardy, 1996). Material that is not burned but rather left in the forest will decay over time, releasing stored carbon into the atmosphere (Harmon et al., 1986). If residues are mobilized for bioelectricity the stored carbon is released in a pulse of emissions at the present time.

The composition and amount of woody residues dictates the flux of carbon in forest ecosystems (Cornwell et al., 2008). Forests are shown to be net carbon sources after disturbance events that cause a reduction in primary production and an increase in woody debris (Clark, Gholz, & Castro, 2004). This includes traditional harvesting which leaves treetops, branches, and unmarketable material as slash. Bioenergy systems can make use of this feedstock for electricity, liquid fuel, and heat production. Other studies have shown that whole tree harvesting specifically for energy production is not an efficient use of energy since this reduces the carbon sequestration rate of a forest by removing trees that could store carbon as they grow or when turned into durable forest products (McKechnie et al., 2011). Residues are a distinctly different scenario as these will decay into GHGs over time if left in the forest. Removing relatively fast-decaying residues and generating electricity with them to offset fossil fuels can help meet short-term climate goals (McKechnie et al., 2011).

The difference in mobilization for energy production and retention of residues in the forest is the temporary sequestration of carbon in the forest residues, which can have implications for short-term climate goals. The decay rate of biomass left in the forest is a main driver of when emissions from residues occur (Giuntoli et al., 2015). Once biomass dies it begins oxidizing and releases CO_2 through decomposition. This is heavily influenced by temperature, moisture levels, and the structure of the biomass (Melin et al., 2009). Material that decays slowly will hold carbon for a longer period and utilizing these materials for bioelectricity has different implications for when carbon is released into the atmosphere.

Mobilizing residues for energy production may provide climate benefits by utilizing the stored carbon and offsetting fossil fuels, which would otherwise be released to the atmosphere through decomposition (Giuntoli et al., 2015). The rate at which these materials decay determines how long carbon is sequestered and can have implications for short-term climate benefits. The climate forcing effect of GHG emissions is determined both by amount of emissions and timing of emissions. A better understanding of how forest residues decay is important for forest ecologists and carbon modelers studying the carbon cycle. There is also importance for life cycle assessments (LCAs) of biomass energy as all carbon must be accounted for in LCAs.

The residence time of materials is commonly measured in turnover time or how long until there is a 100% mass loss (Mackensen & Bauhus, 1999). Material with a shorter turnover time will sequester carbon on the ground for less time and mobilizing these materials will have different impacts than mobilizing materials that persist in the forest for a long time. Understanding the decay of woody materials leads to better predictions of turnover time and estimates for temporary sequestration of carbon in forests.

Past LCAs of biomass energy focused on assessing single projects or theoretical frameworks with assumptions of single decay rates based on simple species compositions (Giuntoli et al., 2015; Pierobon et al., 2014). My research improves on bioenergy modeling by incorporating species specific decay rates for California to capture carbon flows more accurately from decomposition. This has the effect of varying decomposition rates across the state depending on species composition.

The decay will vary by species and climate conditions, which are both location-dependent factors. These outputs will result in a spatial representation of turnover times across the state for forest residues. Turnover times for forest residues can be used to gauge the relative carbon sequestration impacts of mobilizing materials for bioelectricity. The outputs of this research will better define the fate of residues within the context of mobilization for biomass electricity. This data can be used to inform policy decisions regarding the sourcing of materials for biomass energy by defining the counter-factual scenario of residues in more detail.

Background

One of the largest controversies with bioenergy is the idea of carbon neutrality. The emissions created by combustion of biomass for electricity are treated as completely offset by sequestration of carbon from terrestrial vegetation that was used to source the biomass (Berndes et al., 2016). Bioenergy is clearly emitting carbon and other GHGs at the point of combustion, but the landscape is also continuously sequestering carbon through new growth to offset these emissions.

The Intergovernmental Panel on Climate Change (IPCC) tracks emissions from biomass under Agriculture, Forestry, and Other Land Use (AFOLU) as they are primarily concerned with changes to the productivity and carbon carrying capacity of land (IPCC, 2014). Tracking changes in AFOLU should capture emissions from where biomass is sourced while being able to ignore combustion emissions based on the assumption that land productivity is not impacted and the land will eventually re-sequester the emitted carbon (IPCC, 2014). There are concerns that the IPCC methodology for carbon accounting may not be appropriate for biomass energy since the IPCC uses a snapshot in time rather than a projection into the future (EPA, 2014a).

While the IPCC classifies electricity from biomass as carbon neutral, they are also trying to put policy in place that limits global warming to 2° C by the year 2100 (IPCC, 2012; UNFCCC, 2017). Therefore, any policy action should consider not only the total amount, but also the timing of emissions so that these goals can be met. Many studies have shown that under certain circumstances GHG emissions mitigation benefits can be realized by the use of biomass, but carbon neutrality on a 100-year time-scale cannot be assumed for all conditions, due to the variability in feedstock, decay rates, and counterfactual scenarios for each biomass system (Giuntoli et al., 2015; Gustavsson, Haus, Ortiz, Sathre, & Truong, 2015). Furthermore, biomass utilization will almost always result in an emissions pulse, which must be balanced with short-term policy goals.

Life cycle assessment (LCA) of forest products is an internationally accepted approach to determining the overall emission impacts of energy or products that can be used when assessing bioenergy systems (McKone et al., 2011). LCA considers the harvest, transport, processing, and ultimate disposal of a product (McKone et al., 2011). LCAs of forestry and biomass also need to account for time because after biomass is harvested the forest will start to regrow and sequester carbon, offsetting emissions caused by the initial harvest. Many international standards for biomass accounting do not account for time and assume a complete payback of the carbon debt that is incurred upon harvest, making biomass combustion appear carbon neutral (Stephenson & MacKay, 2014). Recent studies suggest the best way to ensure comprehensive accounting is to account for biogenic emissions and sequestration through forest modeling and LCAs (Cherubini, Bright, & Strømman, 2012). Accounting for all carbon emissions and the time of those emissions provides a more realistic framework for assessing biomass power generation.

Piling slash materials is a common practice in forestry operations and quantifying this actions adds to the robustness of the decay modeling (Laird & Pimlott, 2018). No studies on decay have integrated how piling materials post-harvest may affect the decomposition of residues (Barber & Van Lear, 1984; Erickson et al., 1985).

This research on residue decay is part of a larger study of biomass systems in which the residues were created as a side effect from forestry activities. The CBI project is a LCA of forest residues that quantifies emissions from biomass utilization as well as emissions associated with leaving residues in the field. The non-use emissions are driven by decay of woody materials as they release carbon over time. This research will quantify how decomposition varies spatially across the state to inform the non-use case of the CBI LCA.

Literature Review

Types of studies

To explore trends in decomposition rates and parameterize the decay model, a literature review was conducted of past studies on decomposition. This literature review drew on all available sources of data from studies of decomposition with a focus on rates of decomposition, type of material, climatic conditions, and other details about the specific study.

Data from Weedon et al. (2009) was used in this research and expanded upon to include species and genus level variations of decay.

Woody residue decomposition studies typically involve long-term observations or use of a chronosequence approach. Long-term studies are performed over a long period of time and involve repeated measurements and observations of dead organic material as it decays and losses mass or density (Laiho & Prescott, 2004). Chronosequence studies take measurements at a discrete point in time and estimate the age of fallen materials based on visual inspection tying material to a known event, such as windthrow or insect killed trees (Harmon et al., 1986). Many literature values come from chronosequence studies since it is difficult to perform long-term studies due to the length of time required to observe decomposition.

Chronosequence approach is used extensively because it is much easier to perform than a long-term study which requires repeat measurements. Chrono-sequencing does have an inherent bias in that only materials on the ground can be measured, with the fastest decaying materials having already fully decomposed (Pietsch et al., 2014).

Many chronosequence studies use density and volume to estimate total biomass before time of death using standard wood densities. Chronosequence studies also rely on the ability to accurately determine the time since death for the material. In some cases, this is known and attached to a specific event such as harvest, fire, or high wind event.

Long-term studies do exist and provide valuable data on decomposition dynamics for woody material. These were used as sources of decay values when available and as sources of information on the specific drivers of decay (Kahl et al., 2017; Laiho & Prescott, 2004; LIDET, 1995).

Decay Process

Decomposition is the process of organic material breaking down into other components (Harmon et al., 1986). This process is performed by fungi, bacteria, or insects that consume or otherwise separate dead plant material into mineral constituents. Decomposer organisms respire carbon dioxide, freeing the bound carbon in the plant material (Mackensen & Bauhus, 1999). While CO_2 is the main compound that is tracked when measuring decomposition, methane can also be generated through fungal decomposition in anaerobic conditions (Biomass Technology Group, 2002). Methane generation is an area that has not been well researched in the context of forest residues.

Decomposition can be measured by losses in mass, volume, and density. Ultimately mass loss is the most important factor in tracking the temporary sequestration of carbon, but volume and density are also important as these are used to measure decomposition in some studies. Volume and density are easier variables to measure without disturbing or directly affecting the material that is being studied (Barber & Van Lear, 1984; Harmon et al., 2000). Decomposition of slash piles is especially hard to measure given that it is difficult to record the mass of piled material over time. Wright et al. (2017) built a permeable platform to lift and weigh slash piles in two different environments. They were able to compare mass loss of piles over time with this method, although it presents limitations on pile size.

Other studies have measured density, volume, and mass to try to establish a relationship between these variables (Harmon et al., 2000). Density initially decreases but will eventually stabilize, while mass and volume will continue to decrease. Volume is the least consistent measure of a material since it is heavily influenced by environmental events, such as snowfall. A decomposition study of these three measures showed volume to deviate from an exponential model the most and showed the most variability (Harmon et al., 2000). Mass loss dictates overall loss of material to respiration and the temporary sequestration of carbon in woody residues.

Woody material can also break down by physical deterioration from photodegradation and fragmentation. Fragmentation is the process of woody material falling off or becoming separated from a piece of debris. This can be hard to distinguish from other types of mass loss in studies of decomposition (Harmon et al., 1986). Fragmented material has not been biologically decayed but has lost enough density to remain as part of the parent material. Fragmented material then enters the soil column as it continues to decay. The mixture of fragmented material on the forest floor between the litter and mineral soil is also referred to as duff (J. K. Brown et al., 1985).

Soil carbon is relatively stable with most inputs coming from the decay of belowground coarse and fine root material. Long-term research did not find significant changes to soil carbon from the removal of coarse woody debris from the forest floor surface (Powers et al., 2005).

Duff is a mixture of organic materials at the top of the soil horizon, which includes the fermentation (O_e) and humus (O_a) layers (J. K. Brown et al., 1985). Duff is important for fire effects modeling since it will smolder for long periods of time and contribute to smoke and emissions through incomplete combustion (Hille & Stephens, 2005). On a yearly basis, none of this material enters the soil column but rather persist as duff and slowly decays. The mass of duff will increase overtime if there are inputs to the duff and those inputs exceed the yearly mass of decayed duff. Literature is not well developed on the accumulation of duff over time since this is a slow and hard to observe process. Duff has been shown to accumulate slowly in forests through fragmentation and compaction of litter, as mature forests have a thicker duff layer than younger stands (Johnson & Greene, 1991).

Harvest operations and fire are also shown to cause no significant change in the soil carbon content of the upper portion of the soil (Dore et al., 2016). There is limited research on the accumulation of duff since this is a slow and hard to observe process. Duff accumulates over time as a product of decomposition, fragmentation and compaction of litter. Duff has been shown to accumulate slowly in forests overtime as mature forests have a thicker duff layer than younger stands (Johnson & Greene, 1991).

Variables of Importance

The variables that affect decomposition can be generalized into three broad categories; substrate material, the environmental conditions of the material, and access to primary decomposers (Lloyd & Taylor, 1994). All other variables can be thought of as stemming from these basic conditions. Substrate material refers to the chemical composition and mass of the dead plant material that is undergoing decomposition, including the amounts of different nutrients, extractives, lignin concentrations, and other chemical compounds. Lignin, the main component that forms the cell structure of woody material, is relatively hard to break down due to its complex molecular structure (Harmon et al., 1986). Environmental factors have been shown to be impactful on the rate of respiration from primary decomposers that drive decay (Smith et al., 2011).

Environmental conditions in decay modelling are generally simplified to temperature and moisture as these are the two most significant drivers of decay. Contact with the ground and primary decomposers is also shown to have a significant effect on decay rates. This is due to access with the organisms and bacteria that drive decomposition (Edmonds et al., 1986). Enzyme activity and diversity of decomposer organisms are significant drivers of decay.

Species

The chemical composition of the material being decayed can strongly influence the rate of decay (Kahl et al., 2017). Forest residues are composed of different ratios of foliage, bark, sapwood, and heartwood. These components will decay differently based on their nutrient compositions, amount of extractives, and lignin concentrations (Weedon et al., 2009). For example, heartwood decays significantly more slowly than the main tissue due to the higher concentration of extractives, which inhibit decay (Kahl et al., 2017). Woody material therefore requires specialized fungi or insects to breakdown these chemical bonds.

Taxonomic order has also been shown to be a good indicator of decay rates (Pietsch et al., 2014). Species within the same family showed less variation than across different families. Tree species can then be used as a proxy to determine relative decay rates while chemical components of wood are the more important factor.

Gymnosperms tend to have a higher lignin concentration, be more nutrient poor than angiosperms, and have less live tissue. Angiosperms generally have much more live tissues which has a higher proportion of easily degradable materials, such as sugars and starches (Harmon et al., 1986).

While all major nutrients are positively correlated with decay, sulfur and potassium show the strongest relationship (Kahl et al., 2017). Higher amounts of extractives and lignin have a negative correlation with decay rates. These are found in the heartwood and bark of a log and therefore greater amounts of heartwood and bark correlate to lower decay rates. These factors contribute to slower decomposition of gymnosperms than angiosperms. The distinction between angiosperms and gymnosperms is a general trend and not a rule, but these trends appear as broad classes of material.

Size class

Past studies have shown conflicting data on the correlation between size class and decay rates (Mackensen & Bauhus, 1999; Yin, 1999; Zell et al., 2009). One theory is that smaller pieces of woody debris have a greater surface area-to-volume ratio, providing more area for primary decomposing fungi to infiltrate. While this has been shown in some instances, rates of decay do not always follow changes in diameter (Erickson et al., 1985; Harmon et al., 1986; MacMillan, 1988). Lack of a strong relationship with diameter may be partly be due to smaller pieces of wood having a longer duration of low moisture content, which inhibits and stalls decay (McColl & Powers, 2003).

Larger diameter materials have a greater proportion of heartwood, which is generally more decay resistant due to a higher proportion of decay inhibiting extractives (Harmon et al., 1986, p. 198). Large diameter materials are also more likely to hold a more stable moisture level, which is more conducive to decomposition (Gholz et al., 2000).

Some of the variation in decay may also be due to treatment of residues. Trees that are not limbed will have branches attached to the main stem that suspend the resulting woody debris above the ground and decay slower than a main stem that is in contact with the ground (Næsset, 1999). Larger materials are more likely to be in contact with the soil due to their greater weight and soil contact is more clearly related to increases in decay rates (Erickson et al., 1985; Mackensen & Bauhus, 1999). The amount of the decay rate changing is explored in the methods of this study.

The size class distinctions of coarse woody debris (CWD) and fine woody debris (FWD) have been used in past studies to determine differences in decay (Eaton & Lawrence, 2006; Müller-Using & Bartsch, 2009). These are commonly used material size classes in forestry although no formal definition exists for what constitutes FWD and CWD (Eaton & Lawrence, 2006; Woodall & Williams, 2005). Differences in decay rates are more consistently apparent when material is separated into these two size classes (Yin, 1999). The decay rates of CWD and FWD from the same species will be similar to each other since they come from the same parent material (Pietsch et al., 2014).

Vertical position

To estimate the effect of piling slash on decomposition, I created a function to differentiate between piled and scattered material as it is suspended in the air or in contact with the ground (Barber & Van Lear, 1984; Edmonds et al., 1986; Swift et al., 1976). The observed difference in rates of decay are likely due to a combination of available moisture and access to primary decomposers present in soil. Suspended materials are more prone to drying, which can inhibit decay, and are less likely to be inoculated by fungi or have contact with other decomposers which drive mass loss (Kahl et al., 2017).

Material that is buried will decay even faster than material on the surface of the ground because of access to decomposers and more stable moisture levels (Risch et al., 2013). Buried materials are being ignored in this study since residues will rarely end up buried due to forestry operations.

Climate

Temperature and moisture are the most important environmental conditions that effect decay. Temperature dictates the speed of microbial activity and moisture content can inhibit decomposition if it is too low (Kahl et al., 2017). Temperature and moisture act together to modify the decomposition rates of woody debris as it is characterized in decomposition modeling (Sierra et al., 2012).

In a review of functions which effect the decay rate based on climatic conditions, all of the temperature functions increase the decay rate as temperature increases (Sierra et al., 2015). There was significant variation among the different functions with up to a 10x increase in decay at 40 ºC, while climate models show no increase at that temperature. The temperature functions assume inhibition of decay from lack of moisture. Some temperature functions have a drop off past a certain temperature, which is biologically realistic as temperature exceeds levels conducive to decay activity.

Temperature can also be a limiting factor in decomposition when materials drop below freezing and biological processes cease. This has been shown to have significant effects on decay in extreme cold climates and makes modeling of decomposition difficult in these environments (Adair et al., 2008a). This issue is further explored in the discussion section of this paper.

Moisture is a required element for decay and other biological processes to occur (Harmon et al., 1986). High and low extremes of moisture content can affect decay. Too little moisture will inhibit decay by limiting microbial activity. Overly wet conditions can also inhibit decay by creating oxygen poor environments such as in wetlands or bog areas (Smith et al., 2011). Extreme wet conditions would be rare for California forests and most likely only occur in forested marsh areas. California forests would be more prone to extreme drying events, which would slow the decay of forest residues.

There is evidence that when the canopy of a forested area is removed, the remaining residues and mass will decay at a faster rate than materials under an intact canopy (Dore et al., 2016; Finér et al., 2016). When a canopy opens, the forest floor will receive more light energy, increasing the micro-climate temperature. The removal of vegetation also makes more moisture available to the soil and forest floor. These factors can increase decay for recently harvested areas (Yin, 1999). While the direct effects from this have not been well studied and quantified, it should be noted that this effect exists. This scenario would affect forest residues since their generation is always associated with a harvest or thinning, although the degree of canopy cover varies based on the silvicultural prescription.

Aspect has also been shown to be significant in affecting decomposition. This is due to southern aspects (in the Northern Hemisphere) receiving more solar energy than others, increasing the temperature of this land and hastening decay (Næsset, 1999). On a project level analysis, aspect could be incorporated into a decomposition model, although for a more generalized model there is no way to determine where residue will be left. Aspect has been ignored for this study since there is no way to model or predict specific residue locations.

Seasonality has been shown to be more accurate in accounting for decay dynamics related to climate conditions than annual time steps (Adair et al., 2008a; Yin, 1999). This is due to seasons where decay is more active and parts of the year during which almost no decay occurs. Extreme environments or areas that reach sub-freezing temperatures in the winter will most likely experience this seasonality. This seasonality may be hard to detect when annual averages are used.

Many models exist to explain the relationship between temperature, moisture, and decay (Sierra Carlos A. et al., 2015). However, there are challenges to both applying these models beyond theoretical frameworks and integrating these models with general decay models. Many of the environmental models describe the relative change that occurs as climate gradients change, but that do not factor in establishing a base rate of decay.

Models of Decay

The single negative exponential model has been the most widely used decomposition model throughout the literature and has been shown to be representative of decay on a long-term basis (Olson, 1963). Other models exist to quantify decay, but none have been used as extensively as the single negative exponential model.

Expressing decay in terms of a single value k makes this model easy to parameterize and flexible at the cost of being overly simplistic. The processes of decay are complex and while the single exponential is the most widely used it is likely an oversimplification of decomposition dynamics as it assumes a constant rate of decay through time. More realistic models of decay would require large datasets of specific site conditions and would be less feasible because of the amount of information needed. However, single exponential models represent the most studies on decay and provide the largest source of data values to pull from.

A three-phase model has also been proposed and may be a better predictor of decay in specific cases than a more general single exponential model (Adair et al., 2008a). This model is defined by an initially slow phase of decomposition followed by a quicker phase. While this may be closer to reality when modeling decay it is harder to parameterize and lacks enough past research.

Research Objectives

The goals of this research are to examine forest decay rates to inform a life cycle assessment of bioelectricity by modeling decay as a function of species, size class, climate, and vertical position. Variation of species decay is accomplished with a literature review combined with spatial data of forest species and range. Each species will be distinguished by size as two classes representing FWD and CWD. Climate modeling will incorporate local climate conditions into the model of decomposition based on temperature and precipitation.

Decomposition will be quantified with a negative exponential model which uses a single parameter, k value, to characterize rates of decay. The desired output for this work will be rasters of decay values for all forested land of California. These will be expressed as the 50% and 95% turnover times ($t_{0.5}, t_{0.05}$) showing the time at which half and 95% of the material has decayed. The single negative exponential decay model is asymptotic, so $t_{0.05}$ is used as a proxy for virtually all material removed (Mackensen & Bauhus, 1999).

METHODS

Scope of Inference

This research is bounded by the decomposition of forest residues in California. These are materials that are created as part of normal forestry operations, whether that is through forest harvest, thinning, or fuels treatment operations. This boundary exists since these materials could be mobilized for bioelectricity. Surface residues include various size classes and foliage. While foliage is not generally mobilized for bioelectricity it does play a role in the life cycle assessment of bioelectricity.

Duff is an important aspect of this life cycle assessment since it contains carbon in a more stable form than woody residues. A percentage of decayed material is not emitted into a gaseous form but converted to relatively recalcitrant duff.

Decay Model

The decay model is built on a single negative exponential decay model (Olson, 1963). Decomposition mechanisms are characterized through a single decay constant k in the equation:

$$M_t = M_o * \; e^{-k*t} \qquad \text{Eq. 1}$$

where M_o is the original mass, time t is calculated on annual time steps, and M_t is the mass remaining at time t. A single exponential decay function was applied to calculate the mass lost to woody debris over time.

Decayed mass is assumed to enter the atmosphere through cellular respiration or enter the soil organic matter layer as duff (Mackensen & Bauhus, 1999). While there is little research on the formation of duff from woody residues, this mechanism should be incorporated into the decay model as it has implications for carbon accounting and fire behavior. The approach of the Forest Vegetation Simulator (FVS) was used, which moves 2% of the lost mass from exponential decay to duff (Rebain et al., 2015). Duff itself decays along a negative exponential curve at a fixed rate of 0.2%. Duff accumulation and decay certainly varies spatially but there was insufficient data to characterize this in the decay model.

The decay model is calculated on annual time steps as a function of the t parameter. Duff does not directly affect the turnover time of woody residues since its formation comes from mass lost each year through decay.

As forest litter decomposes it becomes increasingly hard to distinguish from duff as it enters the soil column. Therefore, once the litter size class has decayed to 50% of the original mass, the remaining mass is moved to the duff class, creating a one-time spike in inputs. This assumption follows field observations of forest litter interactions on annual time steps (J. Kane, pers. comm., 2019).

Duff is treated uniformly regardless of species composition and will always be considered on the forest floor as opposed to in a pile. Decomposition of duff always has a static k of 0.2% which is not affected by the climate modifier (Rebain et al., 2015). All mass loss from duff is assumed to enter the atmosphere as carbon dioxide although in the forest this may be a source of methane as it encompasses a limited oxygen region of the forest. Duff has been shown to contribute significantly to non-CO_2 gases during fire through smoldering (Urbanski, 2014). The conceptual flow of 1 year of decay is captured in figure 1 below.

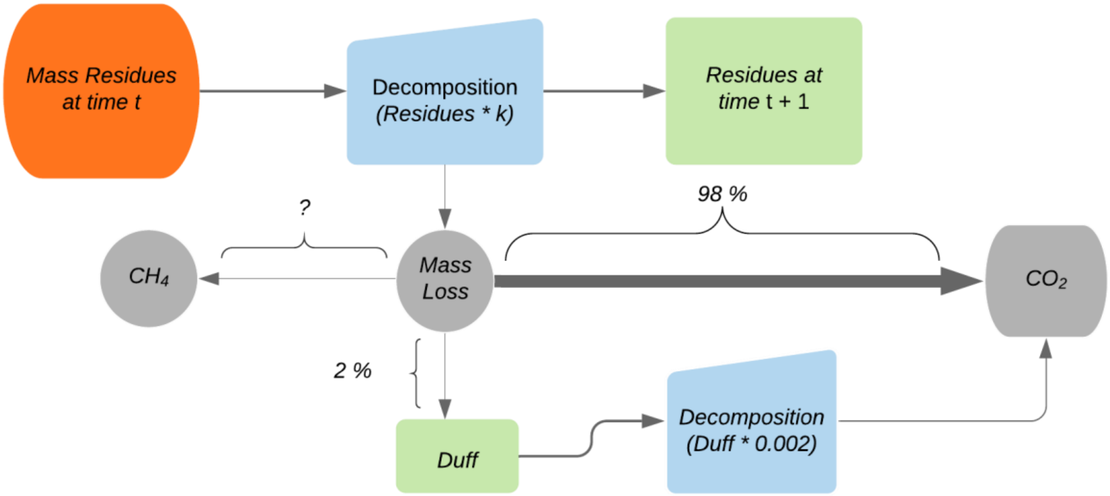

Figure 1: Concept diagram of 1 year of decay model

Due to the different chemical composition of leaf litter and foliage, these materials were treated differently in the decomposition model. Values for foliage and litter were extracted from the species decay database and their mean values calculated based on angiosperm/gymnosperm distinctions. This represents a much coarser approach to varying the decay rate based on available data. The proportion of angiosperms and gymnosperms was calculated for each raster cell of data using the same approach as above and a weighted k value for foliage is calculated.

There has been extensive research and detailed models on how litter decays (Tuomi et al., 2009). Decomposition of leaf litter has been found to vary significantly between angiosperms and gymnosperms, with much less variation within taxonomic families (Pietsch et al., 2014). A coarser resolution was given to litter due to relatively high decay rates and because they are not considered for biomass energy production. Using angiosperm and gymnosperm designation in litter values provides enough resolution of this residue class.

Model Parameterization

A literature review was conducted to gather data from past studies on decomposition of woody debris. Information on species, size class, location, and any specific circumstances from the studies were recorded (APPENDIX A). The literature review was performed by searching all scientific journals available to Humboldt State University. Information about the decay rate of materials was recorded from each study of decay.

Size class comparison

As part of the species database, approximate sizes of the woody debris were recorded. This was done to vary decay not only by species but also by size class of the residues. Size was almost always listed as diameter of material. Some studies only gave a general description of the residues (e.g., logs, branches). Each study was later binned according to fire fuels class distinctions (Table 1). These categories relate to how responsive dead fuels are to changes in moisture conditions and roughly related to fuel diameter (Bradshaw et al., 1984). The fuels classes provide a way to classify qualitative data about the size class of materials as found in the literature. The fuels classes also provide a distinction between FWD and CWD.

Table 1: Fire fuel size classes

Surface Fuel Size (cm)	Fuel Hour Class	Debris Class	Size Class
Litter	Litter	Foliage	Litter
<=0.64	1-hr	Twigs	FWD
0.65-2.54	10-hr	Branches	FWD
2.55-7.62	100-hr	Large Branches	FWD
7.63-22.86	1,000-hr	Logs	CWD
22.87-50.8	10,000-hr	Large Logs	CWD
>50.8	>10,000-hr	Large Logs	CWD

An analysis of decomposition by size class shows a general trend with the progressively increasing size classes, although the increase is not consistent throughout (Fig 2). Large branches have greater decay values than smaller materials, while the smallest materials, twigs, have the greatest decay rates. Differentiating decay along five size classes seems unsupported by this data. While the twigs and large log values match with expectations of large and small diameter materials, the branch and large branches do not.

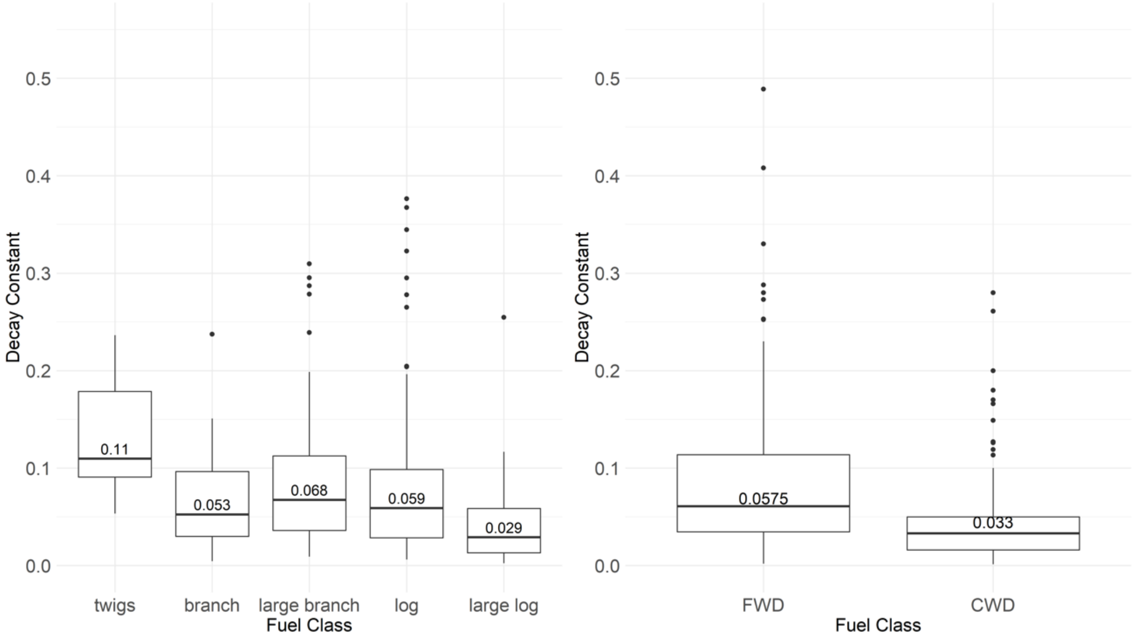

Figure 2: Decay values binned by various size classes

A trend is apparent when materials are separated into FWD (< 7.62 cm diameter) and CWD (7.62 cm and larger diameter) (Woodall & Liknes, 2008). Grouping the data by FWD and CWD produces a clearer distinction between the size classes (Figure 2). In this distinction logs and large logs are CWD and smaller materials are FWD. Based on a two-sample t-test, at a 95% confidence interval there is a significant difference of the decay values from CWD and FWD. The p-value of $1.162e10^{-8}$ is less than 0.05, inferring significance in the difference.

Regression analysis

Based on the previous analysis, decay rates were split and binned by the CWD/FWD distinction so that decay will vary by species and size class. Decay values for all species and size class distinction were not available from the literature. Therefore, missing values were inferred based on a regression of known CWD and FWD decay rates (APPENDIX B). Species that had literature values for CWD and FWD were plotted against each other and a linear model was fit using R statistical software (R Core Team, 2019). The linear model was used to fill in missing values where there was either decay values for CWD or FWD for a species but not both.

Plotting the angiosperm and gymnosperms shows a clear distinction between how these taxonomic orders differ in their decay rates (Figure 3). As the decay rates of CWD increases the decay rates of FWD also increase at a higher rate. The values for angiosperms are generally greater than those for gymnosperms.

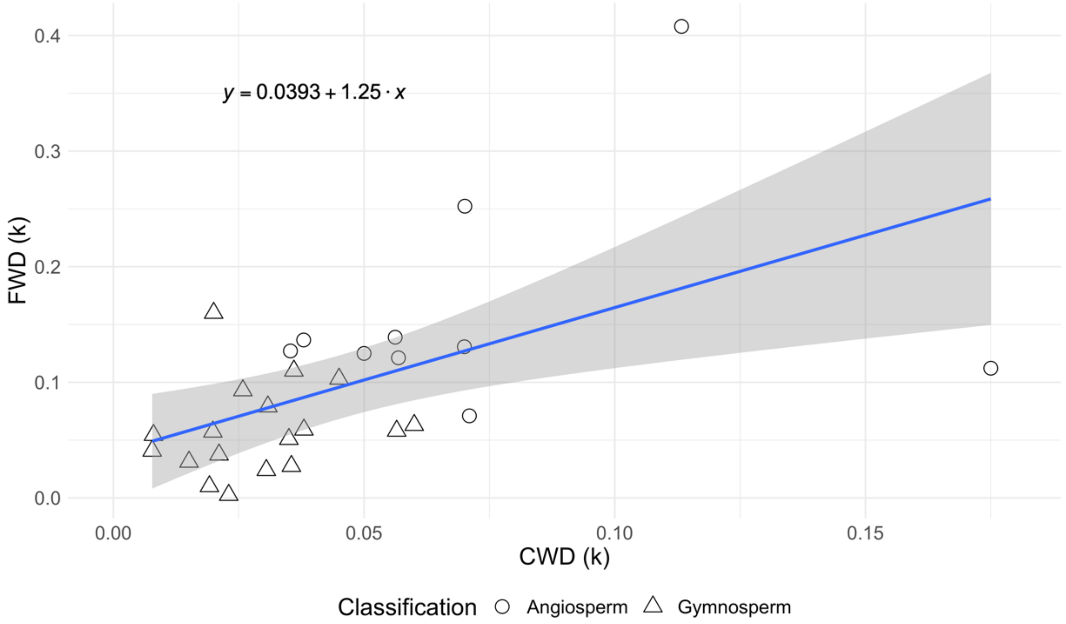

Figure 3: Regression Analysis of CWD and FWD decay rates binned by taxa. R^2 value of 0.279 and p-value of 0.0039.

The linear model was found to produce smaller residuals when calculated over the entire data set as opposed to sub-setting by angiosperm/gymnosperm classification. Sub-setting the linear model by taxonomic order also produced smaller r^2 values and was generally a poorer fit. This is likely due to the larger number of data points from the complete dataset.

A correlation test was also performed on these values to justify the regression analysis. A Pearson correlation test shows a p-value of 0.00386 and correlation coefficient of 0.528, indicating a relationship between the variables. The linear regression model was then used to derive a coefficient value to fill in missing data. The coefficient is the equation for the regression line relating the two variables (Table 2).

Table 2: Linear regression equations used to derive missing values

Regression Equation	To derive FWD values	To derive CWD values
$y = 0.0393 + 1.2535x$	$FWD_i = 0.0393 + CWD * 1.2535$	$CWD_i = \frac{FWD - 0.0393}{1.2535}$

Climate Modifier

Climate modifiers are applied to the decay rates for individual species for all of California. The basic structure of the climate modifier model is a set of functions, representing environmental variables, which affect decomposition constants. This is expressed through the decay function as a factor that multiplies the k constant.

The climate modifier in the most basic form is a coefficient that is multiplied by the decay value for a material.

$$k_m = k * \alpha \qquad \text{Eq. 2}$$

Where α is the climate modifier and k_m is the decay rate with the climate modifier. The climate modifier is composed of functions which capture the effects of moisture and temperature separately.

$$\alpha = f(T) * f(M) \qquad \text{Eq. 3}$$

The functions $f(T)$ and $f(M)$ are multiplied together to get the climate modifier. Many different methods have been used to quantify $f(T)$ and $f(M)$ (Sierra et al., 2015). The approach taken by Adair et al. (2008) was modified for annual calculations for the temperature and moisture functions. This approach was chosen because Adair et al. (2008) used decay measurements from the LIDET long-term study from different climates (LIDET, 1995). Observational decay studies over long periods of time are rare in the literature but provide valuable data on how materials decay in real world settings. The LIDET dataset also represents materials from many different climates across the world. The climate modifier is applied to reflect the spatial variability of climate factors that have been shown to alter the rates of biological decay (Lloyd & Taylor, 1994).

The climate equations create a unitless value which alters the decay rates of residues. The effect of temperature on decay was quantified with the equation:

$$f(T) = \exp\left[308.56 * \left(\frac{1}{56.02} - \frac{1}{(273.15 + T) - 227.13}\right)\right] \qquad \text{Eq. 4}$$

where T is the mean annual temperature in Celsius (Adair et al., 2008). This equation is from the Lloyd and Taylor model to describe temperature effects on decomposition (Lloyd & Taylor, 1994). Equation 4 returns a value of 1 when the temperature equals 10° C. Equation 4 is based off a Q10 equation, shown in equation 5 that describes how biological processes increase at 10° C temperature intervals (Lloyd & Taylor, 1994).

$$Q10 = \left(\frac{R_2}{R_1}\right)^{10C/(T_2 - T_1)} \qquad \text{Eq. 5}$$

The T values are two temperatures while the R values are the two rates of decay. Equation 4 is a variable Q10 function meaning the rate of increase does not stay constant at temperature intervals. Constant Q10 functions are often used to quantify changes in decay, although Adair et al. (2008) found variable Q10 functions to produce a better fit.

The effect of moisture on decomposition is quantified with the equation:

$$f(M) = \frac{1}{1.0+30*\exp\left(-8.5*\frac{PPT}{PET}\right)} \qquad \text{Eq. 6}$$

where PPT is the annual precipitation and PET is the potential evapotranspiration for the site. The $f(M)$ function is based on the CENTURY model to show the effect of water stress on decomposition (Follett et al., 2001). PET is a derived variable calculated using the Penman-Monteith method (Abatzoglou, 2013), which uses a reference crop evapotranspiration to assess relative evapotranspiration. The Penman-Monteith method requires maximum and minimum daily temperature, average dewpoint temperature, wind speed and downward shortwave radiation (Abatzoglou, 2013).

Adair (2008) calculated the climate equations on monthly means for each climate metric. In this application decay is calculated on annual time steps so annual means are used instead.

Neutral climate values

Most of the climate modifier equations that were reviewed have a ‘reference value’ such that the climate modifier equals one. In biological terms, this is the temperature or moisture level where there is no effect, positive or negative, on the decay process versus what would be predicted from the baseline decay model (Figure 4). All other climate values produce a unitless scalar, α, that increases or decreases the decay of materials.

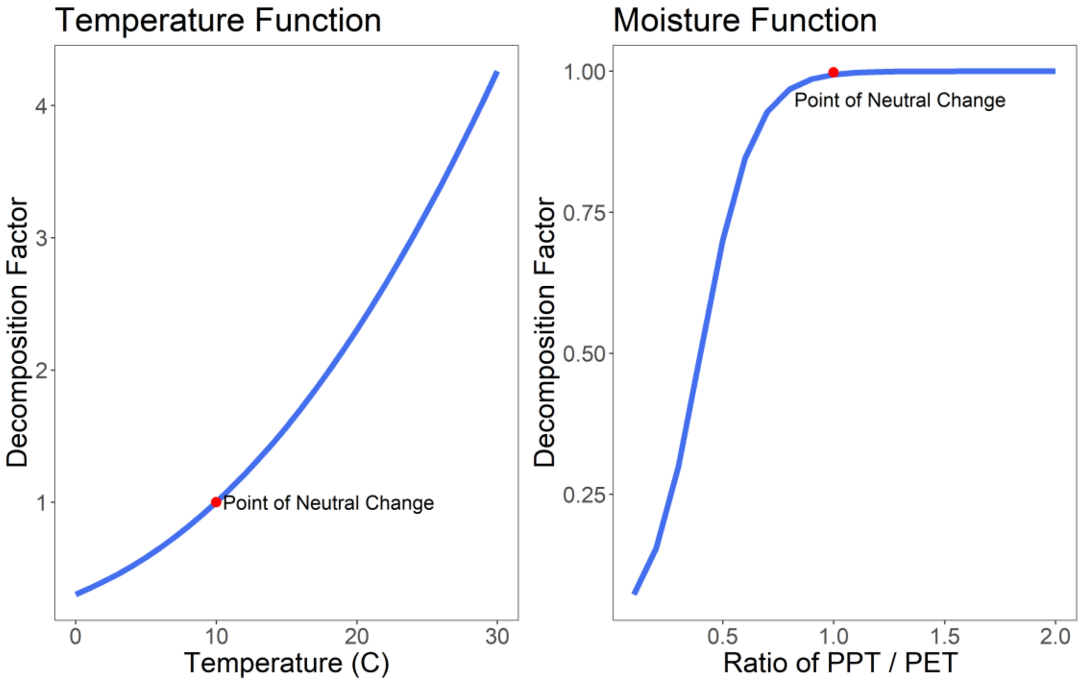

Figure 4: Climate function with points of neutral change

The climate functions always have the same point of neutral change. This presents a problem when applying these functions to species specific decay values. The average temperature and moisture values for the habitat range of each species will fall at different points along the function. For example, a species that only exists in warm regions will have its decay values increased through the temperature function with the opposite being true of species in cold climates. This fails to consider climate conditions that existed when the decay values were first established from the literature sources. These functions must first be normalized to consider temperature and moisture conditions for species at each study location.

Climate data

All climate data used in the $f(M)$ and $f(T)$ equations come from the gridMET data products (Abatzoglou, 2013)[1]. This data is made available through the University of Idaho and is open to the public. The gridMET data products are at a spatial resolution of 4km for the contiguous United States and are available at a daily temporal resolution.

The data used represents an 11-year average from 2007 through 2017 for mean annual temperature, potential evapotranspiration, and annual precipitation. The 11-year time span was chosen to capture recent weather trends and to smooth yearly anomalies. California experienced a severe multi-year drought during this time where temperatures were above average, and precipitation was below average. These conditions may be more representative of the future as California experiences climate change.

These data are used in the $f(M)$ and $f(T)$ equations to produce two rasters which quantify the effects of temperature and moisture on decay. These two rasters are multiplied together to produce the α climate modifier value. Areas that are warm and wet will have an increase in decay rates, while areas that are cold and relatively dry will have decreased decay. Areas that are a mixture of these climate conditions will produce more neutral changes.

Applying the statewide climate modifier directly to the k values derived from literature could have the effect of double counting the impact of climate on decay. This is because the k values themselves are based on measurements taken in non-standardized

---

[1] Data download link:
http://thredds.northwestknowledge.net:8080/thredds/reacch_climate_MET_catalog.html

climate conditions. For example, some species are only found in cold and relatively dry areas of California. The empirically derived k values for these species will most likely also have come from cold and dry areas. Applying a climate modifier will have the effect of further decreasing the decay values for these species.

The approach was taken to treat k_m as the literature derived decay values (Equation 7). Using climate information about each study location, the C_m was calculated with the $f(M)$ and $f(T)$ equations. This approach acknowledges the inherent effect climate has on decay and serves to normalize literature-derived decay values before applying California specific climate modifiers. The k_i value is derived with Equation 7 using the calculated C_m and the literature k_m, for each literature decay value.

$$\frac{k_m}{C_m} = k_i \qquad \text{Eq. 7}$$

This approach requires climate information about each literature-derived k value so the $f(M)$ and $f(T)$ equations can be parameterized and results in a climate normalized value, k_i. Many of the studies on decay record the MAT and PPT for the study site. If these climate metrics were not recorded the location of the study was used to extract the MAT and PPT using a combination of Google Earth and QGIS. While exact locations were not always available, the gridMET data has a 4km resolution so exact specificity is not required. The climate values come from the same eleven-year averages used to parametrize the climate functions. None of the decay studies reported PET as this is a derived metric, so the preceding methods were used to extract all these values.

Some of the studies on decay occurred outside the United States while gridMET data only covers the contiguous US. All the studies outside the US report MAT and PPT, but do not report PET. For these studies, data from the USGS Global Data Assimilation System (GDAS), which reports Daily Potential Evapotranspiration[2]. The data was processed and aggregated similarly to the gridMET data with the same temporal resolution.

The climate normalized decay values are averaged based on genus, species, and size class. These mean normalized k values are then applied across the species range in California and the climate modifier changes those values based on that range. The k value at each location represents a weighted average of the species mix. Most of the angiosperm species were grouped based on the genus level as no California specific species values were found in the literature. This most notably affects oaks (*Quercus*) as they are the dominant angiosperm found in California.

Constructing the climate model

The CBI project uses modeled data of the residue base of California forests under various harvest scenarios. The harvest data was prepared by a team of engineers at the Natural Resource Spatial Informatics Group (NRSIG) and breaks residues into various size classes and amounts under different canopy removal scenarios as modeled using the Forest Vegetation Simulator (FVS) (Comnick & Rodgers, 2018). This modeled data uses

---

[2] Data to determine the PET for studies outside the US was downloaded from the website: https://earlywarning.usgs.gov/fews/product/81

the GNN Structure Maps created by the Landscape Ecology, Modeling, Mapping, and Analysis (LEMMA) research group (Ohmann & Gregory, 2002). The NRSIG data is used for establishing the species composition of California forestland, which plays a significant role in the decomposition characteristics of potential residues.

The equations used to generate the climate modifier map were developed from the LIDET dataset to model decomposition of woody debris in forestland and was shown to be least accurate in extreme climate conditions.

The basic flow of constructing the climate model is shown in figure 5. To calculate climate values of species at spatially explicit locations, the NRSIG data was parsed into individual rasters showing the proportional abundance of a given species in each cell of data as a value between 0 and 1. These rasters also show the geographical range of every species in the data.

For each species or genus, the climate-normalized decay value is assigned to all locations across California. These decay values are then modified by the α value which represents climate conditions of California based on an eleven-year average. For example, if a study of (*Pinus ponderosa*) ponderosa pine shows a k of 0.05 and the climate conditions from that study produce a α of 0.7, the climate normalized k would be 0.714. Ponderosa pine exists primarily in dry areas, so it will likely always have a α of less than 1. The climate-normalized k values for ponderosa pine from all studies are averaged together to produce k_i. This value is applied to the range of ponderosa pine across California and then modified by the α in each location across the state. If the k_i is

0.714 and the α is 0.7, the k_i is returned to 0.05, meaning ponderosa pine in that area of California exists in similar climate conditions to the literature derived study site.

This produces spatially variable decay rates for each species based on climate conditions. These rasters were then combined as a weighted average into a single decay raster based on proportional abundance of a given cell. These steps were taken for CWD and FWD to produce two rasters showing each size class of residue.

A simplified approach was taken with foliage. The decay rates of foliage are only varied by the angiosperm/gymnosperm distinction due to available data. The proportional abundance of angiosperms and gymnosperms was calculated for each cell and the previous steps were repeated to create spatially variable decay rates of foliage.

An inherent effect of forest harvesting is that the canopy opens and more solar radiation and wind will hit the forest floor, which has significant effects on microclimates and can lead to an increase in decomposition of residue materials (Finér et al., 2016). This effect is not captured in this methodology due to a limit in data and difficulty in quantifying this effect.

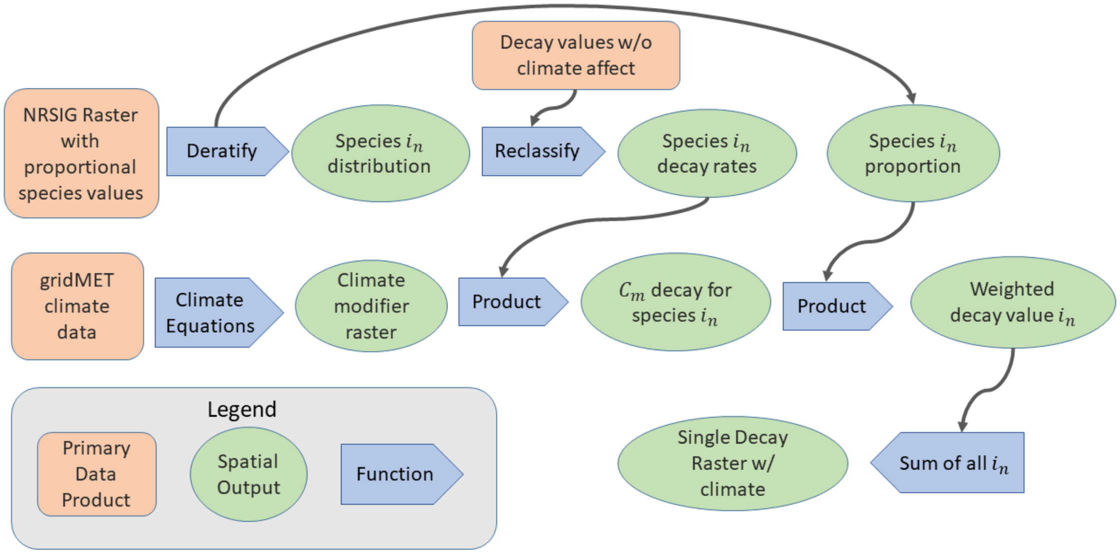

Figure 5: Conceptual workflow of climate modifier pathway

Weighted Average

The resultant database has decay values for every species of every raster cell that has biomass resources. There are some raster cells that have no residues associated with them and are not represented in this database.

Decay constants vary by species, and species composition varies by location. The decay constant, k_n, was calculated for each raster cell as the weighted average for the mix of species present. The weights for each species were calculated as the proportional abundance by basal area (BA) for each raster cell. Using the calculated k_n values which account for climate, a weighted average value was calculated based on the proportional BA of the species in each cell.

$$\sum_s \frac{\sum BA_s}{\sum BA} \qquad \text{Eq. 8}$$

where $\sum BA_s$ is the sum BA for a given species in a raster cell, and $\sum BA$ is the sum BA for all species in the same cell. For each cell Equation 8 sums to 1. The sum BA for each species in each raster cell ($\sum BA_s$) was calculated from the residual tree list. Dividing a species aggregate BA by the sum BA for each cell ($\sum BA$) gives the proportional abundance of that species. For the state, (*Pseudotsuga menziesii)* Douglas-fir, (*Pinus ponderosa)* ponderosa pine, and (*Abies concolor)* white fir compose the three most prominent species in the state (Figure 6). Gymnosperms are also dominant as a category, comprising most of the tree area. Figure 6 only shows species which make up at least 1% of the total proportion and cuts off the long tail of less common species.

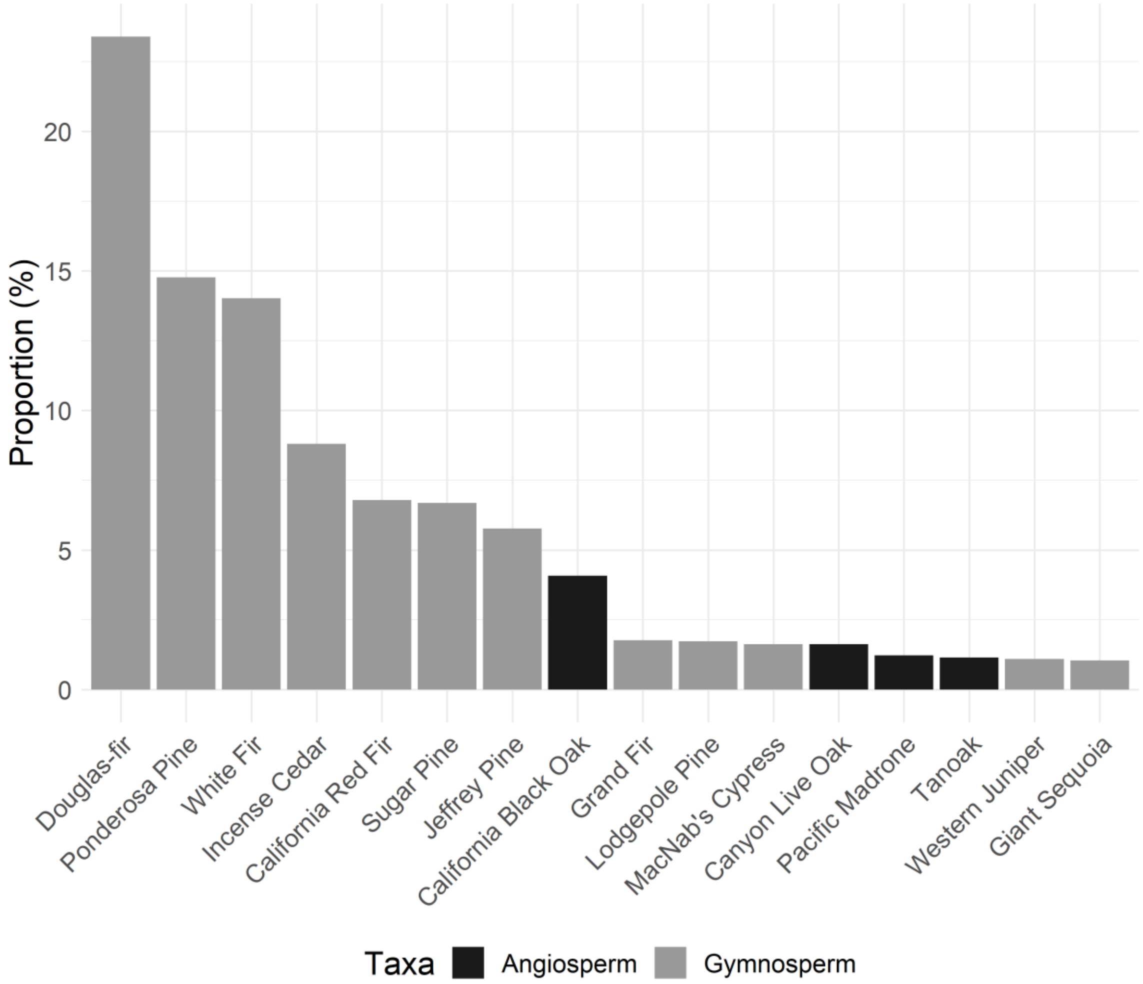

Figure 6: Species proportions of California species by relative proportion of total basal area. Top sixteen species are shown which all comprise at least 1% of total proportion.

The species listed in the NRSIG data were matched to available decay values from the literature review data based on taxonomic order. The NRSIG data has entries for 115 species representing 43 different genera, not all of which were represented in the literature review data. These are in the long tail of Figure 6, which are not shown. Species that did not have literature values were placed in an “other” category that varied by angiosperm/gymnosperm designations. All species in the NRSIG data were categorized into a species, genus, family, or other category which relates to the decay database. While the “other hardwood” category represents incomplete data, the major forestry species are the best represented in the literature. All the species placed in “other hardwood” represent a small overall proportion of potential residues.

Piled and Scattered Distinction

Pile decay was modeled by dividing materials into a portion that is in contact with the ground (Ground Contact or GC) and a portion that is elevated from the ground (Above Ground or AG). Piled materials decay slower because of reduced contact with primary decomposers and ground moisture. To determine the fraction of piled material in these two classes, the first step is modeling pile shape.

Slash piles have been shown to vary widely depending on the logging system used, but generally resemble a paraboloid shape (Figure 7) (Wright et al., 2017).

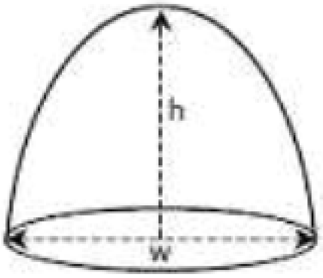

Figure 7: Paraboloid shape of slash piles. H represents the height of the pile and W represents the width (Hardy, 1999).

All slash piles are treated as identical paraboloids for simplicity. Pile size was approximated as a geometric paraboloid with equation 9, where H is the height and W is the width of the pile (Hardy, 1999).

$$V = \frac{\pi * H * W^2}{8} \qquad \text{Eq. 9}$$

To model slash piles a typical height and width are needed. Miller & Boston (2017) measured slash piles from different harvests throughout Oregon and reported the number of piles, total pile footprint, and pile volume. Since they did not report width, this variable was calculated using equation 10, based on the reported area of each pile.

$$W = \sqrt{\frac{area\ per\ pile}{pi}} * 2 \qquad \text{Eq. 10}$$

Equation 10 was solved for H. Having a typical height measurement allows material to be classified into the two groups AG and GC. The average pile height was assumed to be roughly 3.1 m (Miller & Boston, 2017). This number is in line with previous research concerning typical maximum pile heights for forestry practices (Winterbourne, 2016).

It is assumed that piled material within one foot of the ground is in reasonable contact with the ground and is considered GC. A second paraboloid is calculated which does not include material one foot from the ground and subtracted from the full pile to get the volume of material in contact with the ground (Equation 11).

$$GC = V - \frac{(pi*(H-D_g)*W^2}{8} \qquad \text{Eq. 11}$$

In Equation 11, D_g is the distance from the ground, which is set at one foot. The AG material is then calculated as the difference in the GC and the whole volume, shown in equation 12.

$$AG = V - GC \qquad \text{Eq. 12}$$

Using a typical height of 3.1 m and a distance from ground as 0.3048 m (1 ft) the AG and GC percentages are 89.1% and 10.9%, respectively. These proportions are dependent on the distance to ground value, which is a qualitative choice. A rough approximation by visual inspection was proposed as 80% AG and 20% GC (Barber & Van Lear, 1984).

Altering decay

Some k values from literature were only identified to genus level of specification. For these species, a genus-specific k value was calculated and applied to all species of that genus. This was most prominent in angiosperms, which tend to have larger numbers of species in a genus. For example, the literature does not contain studies on each

Quercus species found in California, so a *Quercus* decay value was calculated from a mix of different species.

A coefficient is applied to the weighted average decay rate for AG material to characterize the slower decay rate. Piled material is assumed an even distribution of species, For each study measuring the effect of vertical position on decay, the mean observed decay rates were put into a ratio of AG/GC and then averaged together to find a single coefficient (Table 3). The resultant coefficient can be used in an exponential decay equation as a multiplier to the decay rates of debris to capture the effect of piling slash.

Table 3: Decay ratios of Aboveground (AG) and Ground Contact (GC) materials from past literature

Reference	**AG/GC**
Garret et al. 2010	0.691
Mattson 1987	0.709
Swift 1976	0.664
Edmonds et al. 1987	0.741
Erickson et al. 1985	0.721
Barber & Vanlear 1984	0.775
Naesset 1999	0.748
Mean	**0.721**

As opposed to tracking two classes of material that decay at different rates, a weighted average approach was taken for piled material. The decay value for piled material is altered based on the proportions of AG/GC material and the piled coefficient,

P_c, of 0.721. Equation 13 shows the weighted average approach for piled material based on the calculated proportions of AG and GC.

$$k_p = (k * P_c * \ AG\%) + (k * GC\%) \qquad \text{Eq. 13}$$

As piles decay the percentages of AG and GC remains the same in the model, although this would not be true in the field. Tracking changes in pile shape is not feasible for this study as these equations are designed to give a first order approximation of the differences in piled material versus scattered material. The effect of tarping slash piles is also not characterized, although this can have significant effects on the moisture content of the piled material (Afzal, Bedane, Sokhansanj, & Mahmood, 2010).

RESULTS

Climate Rasters

The values in the climate raster are scalars that are used to modify the decay rates of materials and range from 0.071 to 1.887 (Figure 8).

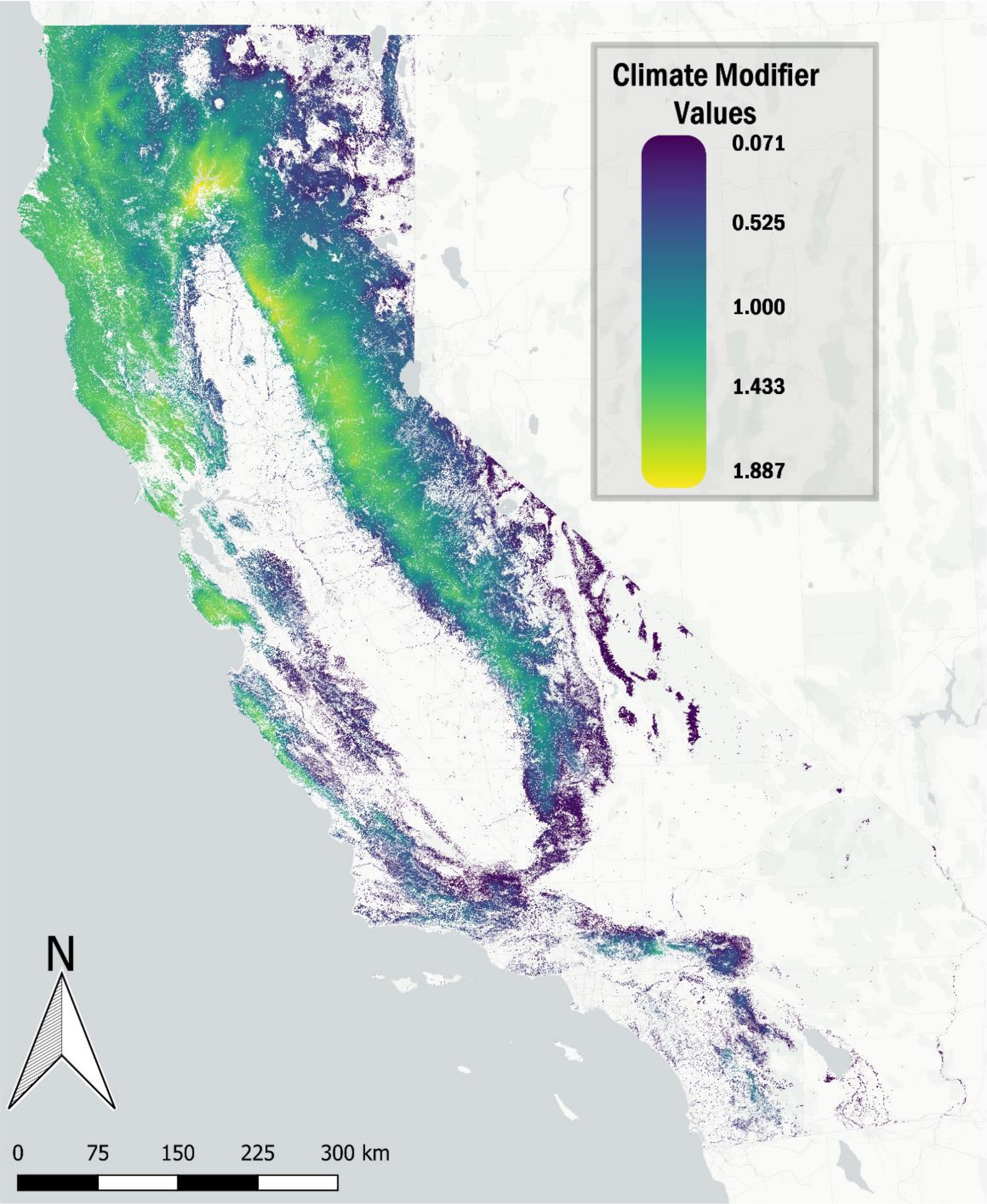

Figure 8: Climate modifier value variation across the state of California. The climate modifier values alter the decay rates for residue materials at each location. These data were derived from gridMET climate data using equations that quantify the effect of temperature and moisture on the rates of decay.

The resultant climate raster shows some areas of the state as having a near zero climate modifier value (APPENDIX C). This occurs mostly in parts of the state that have low yearly totals for precipitation and are classified as desert regions. The eastern and south eastern areas of California as classified as types of desert while the rest of California is classed as a Mediterranean climate. While most of the low values occur in desert regions, some of the low values occur in the Mediterranean climates east of Santa Barbara.

Site Specific Decay Rates

Without the climate modifier, all the decay values for each species would be a single value, but the climate modifier has the effect of varying decay spatially and showing a measure of the range of each species.

The range of decay values for each species reflects the different climate conditions of each species. Estimated mean decay rates varied widely in the 10 most prominent species, ranging between 1.0% and 6.6% annual loss. With the climate modifier applied to each species the decay rates range between 0.3% - 11.3% (figure 9). Coast redwood (*Sequoia sempervirens*) is added to figure 9 since it is of interest to restoration projects.

While California Black Oak (*Quercus kelloggii*) and Canyon Live Oak (*Quercus chrysolepis*) are the most prominent oaks species in California, no species-specific decay rates were found in the literature. Therefore, only genus level summaries can be made, which may not be representative of these California species.

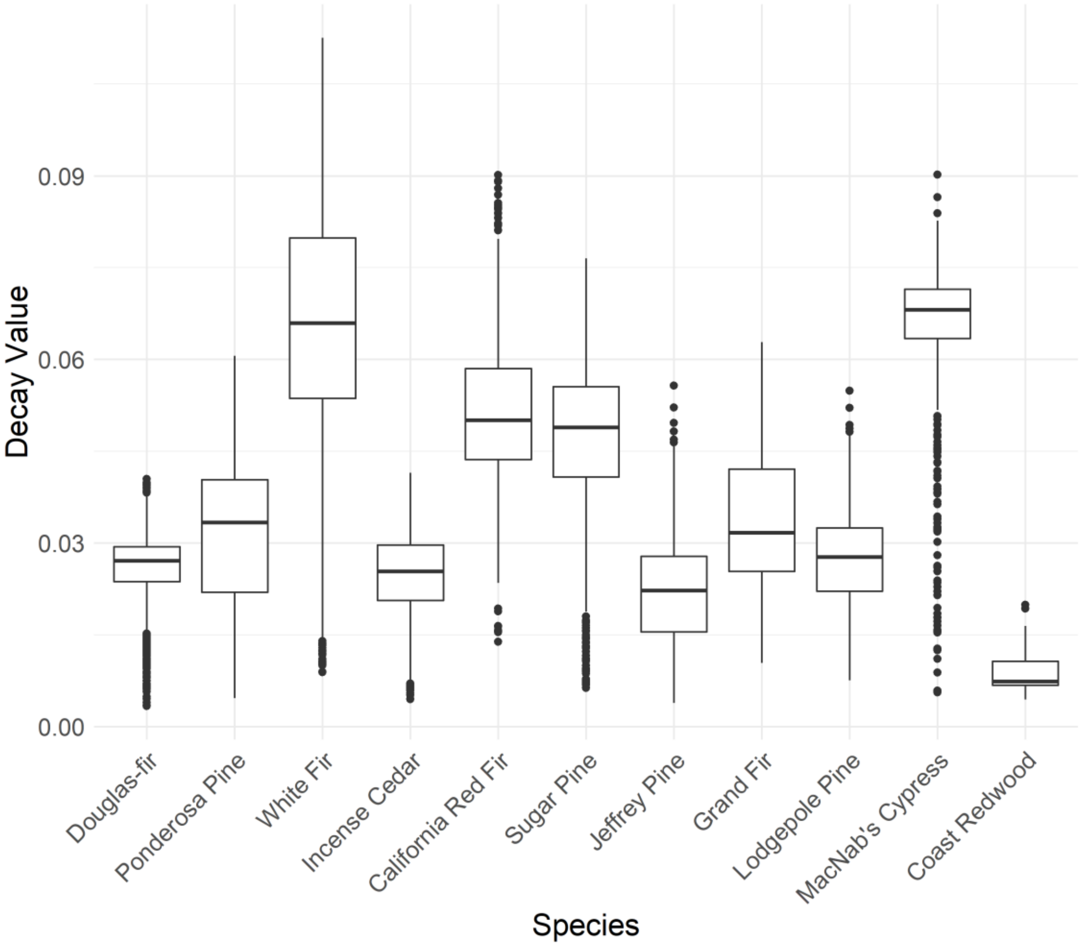

Figure 9: Variation in decay rates for the most prominent species in California. The middle line is the median decay rate, and the limits correspond to the first and third quartiles. The lines extend to 1.5 times the interquartile range and outliers are plotted individually beyond those values.

Most of the conifers have a tighter range of decay values than the broadleaf oaks. While differences amongst species are important in differentiating decay values and residence times, this data suggests that the climate and the broader classification of taxa are the more important factors in decay rate. MacNab cypress (*Cupressus macnabiana*) has a prominent set of outlier values of low decay. This may be due to the overlap in range with the oak species in dry areas.

Piled and Scattered Distinction

The results of applying the climate modifier methods are three composite rasters showing decay values for CWD, FWD, and foliage. These rasters show expected annual rates of decay for different size classes of material based on the species composition and climate conditions. While decay rates are useful to some individuals, a more concrete definition of the impacts of decomposition is the residence time of materials on the ground. Residence time is a measure of how long material is on the ground and how long carbon is stored in those materials.

Residence time can be derived from the decay rasters by dividing the natural log of the mass of residues at a given time step by the decay rate. Residence time is commonly expressed in either 50% or 95%, with 95% being considered the maximum amount of material having been decayed. Residues will never reach zero with a negative exponential equation so 95% reduction can be considered near-full decay of material. The 50% residence time is a measure of the half-life of residues.

The mapped residence time values show spatial variation across California (Figure 10). This variation is driven by the different species composition and climatic drivers of decay. Figure 10 has two legends to show the 50% and 95% residence times. The equation is the same for both residence times, so the spatial distribution does not change, only the values. The lowest values appear on the coast and in the low elevation areas of the Sierra foothills. The highest values are found in the high elevation areas of California and east of the Sierra Mountain Range.

Figure 10 has values that fall above the 95th percentile removed as these represent outliers in the data. The outlier values are a product of low decay rates for CWD and climate modifier values near zero. Again, these areas reflect more extreme climate conditions which were shown to be least accurate in the original LIDET dataset in predicting decay rates. These are alpine, high desert, and areas of Southern California which are dry much of the year and produce unrealistic half-life values.

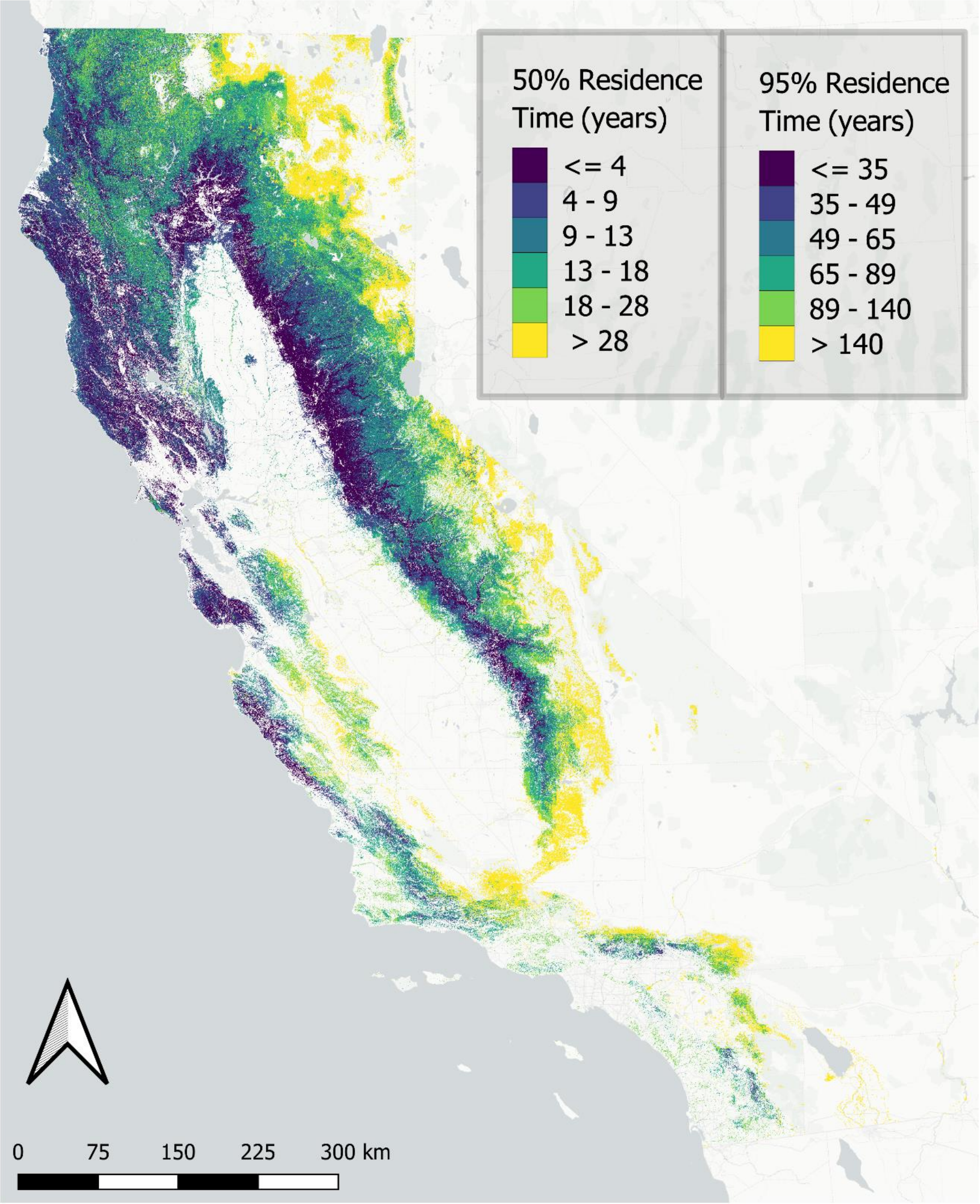

Figure 10: 50% and 95% residence time for coarse woody debris (material > 7.62 cm diameter) across California. Residence time is the length of time material is expected to persist in the environment.

These data can also be expressed as a histogram to show the relative amounts of each value (Figure 11). Figure 11 shows the distribution of 50% residence time for CWD. The data is right skewed with some very large values in the extreme right of the graph. There appears to be a hump in the data, but that is only visible due to the log scaling. The 95th percentile cut-off is also shown as this figure represents the full range of the data.

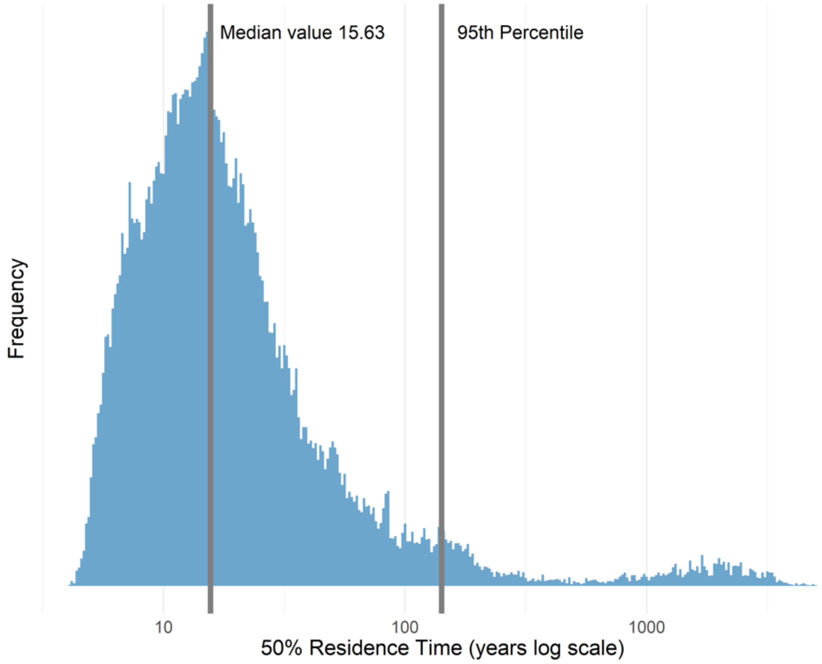

Figure 11: 50% Residence time histogram of coarse woody debris values. The median value and 95% percentile are shown to illustrate the distribution of values. X-axis is in log scale.

A similar figure shows the distribution of values for FWD (Figure 12). The right tail of the data is much more prominent with a more even distribution of the higher half-life values. The median value of 8.00 is roughly half that of the CWD values.

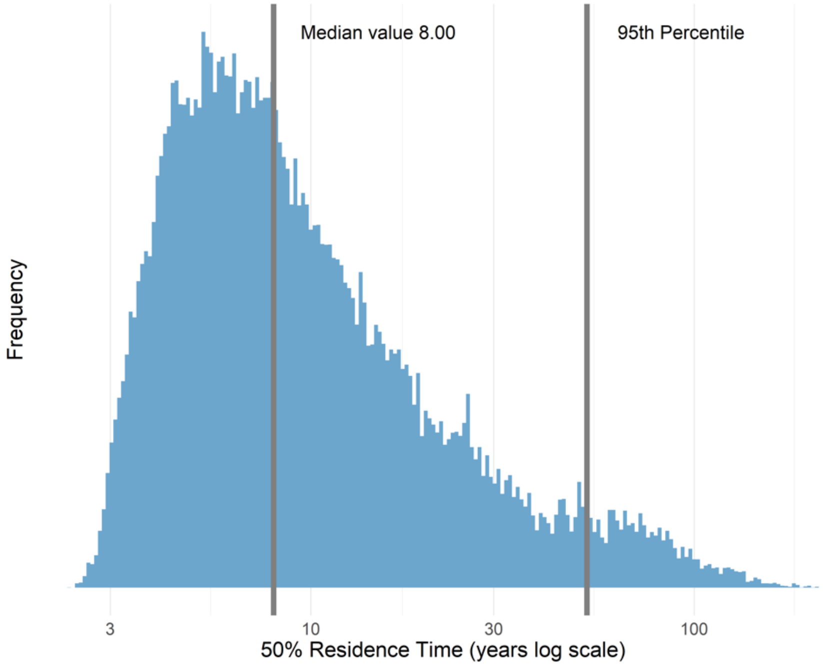

Figure 12: 50% Residence time histogram of fine woody debris values. The median value and 95% percentile are shown to illustrate the distribution of values. X-axis is in log scale.

The distribution of litter residence times represents the lowest values with a median value of 2.48 years (Figure 13). While the maximum value falls just above 30 years, the 95% percentile value is about 13 years, less than half the maximum.

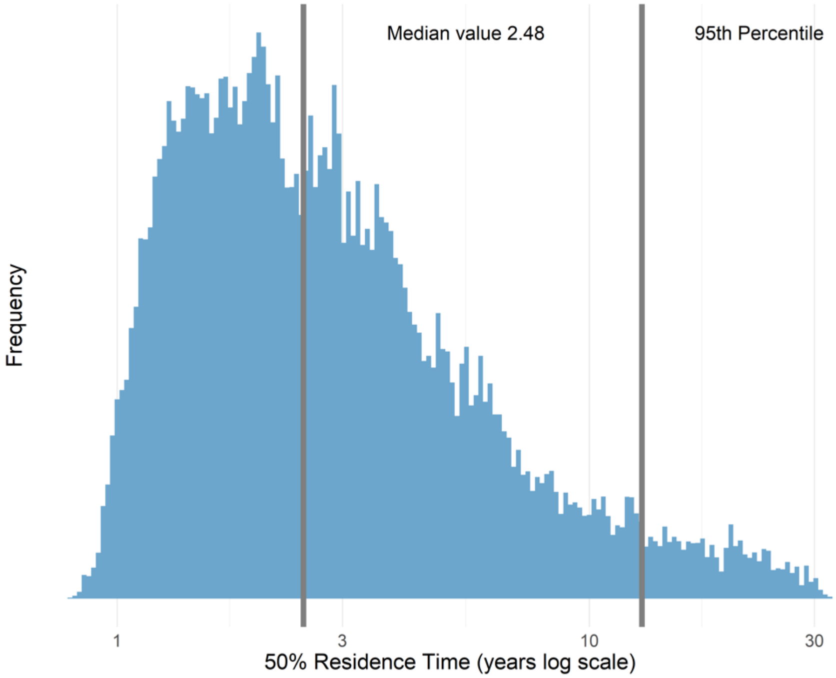

Figure 13: 50% Residence time histogram of litter values. The median value and 95% percentile are shown to illustrate the distribution of values. X-axis is in log scale.

The residence time values can be further modified by applying the pile scenario to these materials. Piling materials slows the rate of decay by limiting contact with soil moisture and primary decomposers, causing residues to persist in the forest for longer. Assuming a percentage of material in any given area is piled, a new residence time can be calculated by apply the piled decay rate to each decay value

The various residence time metrics under scenarios of CWD, FWD, and piling were quantified (Table 4). Piling materials does not change the shape of the distributions shown in figure 11,12, and 13. and instead only changes the residence time values. There is a large discrepancy between the median and mean values, especially for CWD. The mean value is greater than the 75th percentile for the CWD cases highlighting how the maximum values skew the data. Again, these are outlier values caused by edge cases in the climate modifier values.

Table 4: Summary statistics for residence time (years) of CWD and FWD for scattered and piled materials.

Metric	**CWD 50%**	**FWD 50%**	**Piled CWD 50%**	**Piled FWD 50%**	**CWD 95%**	**FWD 95%**	**Piled CWD 95%**	**Piled FWD 95%**
Min.	4.1	2.2	5.6	3.2	17.7	10.1	24.0	13.7
25th Percentile	9.9	5.2	13.3	6.9	42.9	22.4	57.0	29.9
Median	15.6	8.0	20.8	10.6	67.4	34.1	90.2	45.9
Mean	75.5	14.6	102.7	19.8	331.9	62.9	443.9	85.2
75th Percentile	27.7	14.9	37.5	20.1	120.6	64.1	160.5	86.2
95th Percentile	143.8	53.9	192.2	72.4	610.5	229.9	791.2	311.8

DISCUSSION

Key Findings

The approach taken to apply a climate modifier to estimate site-specific decay values is innovative in this field. This has implications for bridging theoretical work done on how temperature and moisture effect decay and how these models are applied to residues. Decay values normalized based on the climate conditions from the original study. Any further studies of decay should include climate information as that has been shown to have a large effect on decay rates.

The residence time rasters can be used to inform decision makers when considering whether to mobilize residues for biomass energy by identifying areas of the state where material will persist in the forest for relatively short periods of time and therefore sequester carbon as dead woody biomass for shorter periods of time. Taking materials from areas with longer residency times and releasing that stored carbon through energy production will have a different effect when trying to meet near-term climate goals. The decomposition of residues is only one part of the decision when considering forest residues for biomass energy production, but this tool helps inform the fate of carbon as forest residues.

The climate modifier has a large effect on the overall decay of materials. *P. menziesii* has a mean decay rate of 2.1%, but with the climate modifier applied ranges between 0.3% and 4.0%. Douglas-fir exists in a relatively tight climatic range within

California, although the range across North America is quite large and spans many different climates. *Abies concolor* (white fir) has a much larger range of values between 0.9% and 11.3% while the mean decay value is 6.6%. The climate modifier has a near doubling effect in some areas and reduces the decay rate to close to zero in others.

This research also resulted a tabular database of decay values that have been corrected for the climate that they were measured in. These values can be useful to land managers and researchers as they represent a new approach on how decay is measured with the explicit acknowledgement that climate is always a factor in how materials decay.

Some parts of California are extremely dry and hot for most of the year. Using yearly averages may be masking these areas from showing times in which the precipitation is greater than the overall evapotranspiration rate, facilitating decay. There may be more of a ‘decay season’ in areas that experience seasonal droughts, although this concept is not explored in this study. Areas that are warm and have enough moisture have the highest climate modifier values while cold and dry area have the lowest climate modifier values. Areas that are extremely dry will also have low climate modifier values regardless of the temperature in these regions. These areas should be examined with truthing data to validate these outlier results to better parameterize the climate model.

A method for differentiating decay based on piles was also developed in this research. The mean values for piled residues are 3.7% and 7.0% for CWD and FWD, respectively. Past research measured piled decay at 2.7% for a site in Washington State and 6.4% in New Mexico (Wright et al., 2017). The values calculated in this study are slightly higher than found by Wright et al. (2017), especially considering any pile will be a mix of CWD and FWD but seem reasonable given the effect of climate on decay rates.

Within the model parameters explored in this paper, the fastest decaying materials are generally angiosperm species and small diameter residues that would otherwise be left scattered on-site. In many harvest scenarios, all the biomass from angiosperm species will become slash.

The cause of the difference between angiosperms and gymnosperms is a product of chemical composition and physiological differences in how these taxa are structured as explored in the literature review. gymnosperms have higher amounts of resin and extractives that are shown to inhibit decay rates (Kahl et al., 2017). The difference is also driven by the carbon/nitrogen ratio which is generally higher in gymnosperms.

Large harvests may also influence decay due to the amount of debris that is entering the ecosystem at one time. Much of decay is driven by the nutrient content of materials and a large influx of woody debris will increase the carbon/nitrogen ratio possibly slowing overall decay. Past research on decay is not exclusive to large harvests and reported values may change in different site-specific conditions. Incorporating this into the model would require more detailed data on the type of harvest that generates residues.

One concern of this study is that it assumes an even distribution of residue generation. While a small overall proportion of total mass is made up of broadleaf angiosperms, these species are often cleared completely in forestry operations with all their mass going to residues. The data from NRSIG does not capture this action and residues are generated evenly amongst all species. Higher resolution data could capture this affect, which may increase the number of angiosperms in forestry residues.

Sources of Uncertainty

The decay rasters were created based on a proportional species basis. Since residues are generated from forestry activities, the mass of some species, which are not marketable, will go entirely to residues. This will lead to a non-even proportion of residues created to species present. Angiosperms, which are generally not merchantable, may have a higher proportion of their mass become residues, although they represent less overall mass in commercial forest plots. Future work could utilize species preference when modeling how residues are created to show forest activities more accurately.

Further, angiosperm data for California species was not sufficient to estimate decay of these residues with certainty. This is most important for oak species of California, with most of the literature review data sources coming from the Eastern US or Europe. Data is instead summarized at the genus level, which has more limited applicability for California species. The broader conclusion is that angiosperm species have generally higher decay rates than gymnosperms.

Areas which experience drought-like conditions at some point in the year are the most likely to have seasonal decay. Many of the outlier decay values come from these dry regions where the annual evapotranspiration is far greater than the available moisture. This model could be improved upon by calculating decay on monthly time intervals with finer resolution weather data. The outlier values may also be due to a lack of observations in these hot and dry climates. Validating the model against observations in these climates would also lead to a more robust model.

The climate equations used were tested against the LIDET dataset, which is a spatially extensive long-term study of decay which isolated climate effects by using a consistent size and tree species in the study (LIDET, 1995). While the equations are based on empirical observations, they are not specific to California climates. Furthermore, localized climate conditions vary significantly throughout the year and an annualized average for any climate metric may not represent the actual climate conditions. Adair (2008) used monthly averages in their work, which would give a higher resolution of temporal differences in how materials decay.

The larger CBI project is concerned with mobilization of residues for biomass energy generation to deal with the waste products of forestry activities. Many of the forestry operations that produce residues create clearings in the canopy, which then let more sunlight and energy onto the forest floor. This invariably increases the microclimate temperature for areas that have recently been clear-cut or have some level of canopy removal (Finér et al., 2016). Further, stand density may play a role in decay rates because of sunlight reaching the forest floor and interception of precipitation by the canopy. These are factors could be accounted for and quantified in future decay modeling.

Harvesting or thinning stands may also affect the available moisture and decay rate of residues. In some areas, thinning stands has been shown to have no effect on seasonal surface residue moisture, while in other climates these differences are significant (Estes et al., 2012; Finér et al., 2016). Capturing this effect in a decay model would likely require finer temporal resolution or better information on what type of harvest or thinning is occurring.

Since weather data comes from a gridded dataset at 4km resolution, changes in microclimate due to harvest scenario are not reflected in the results. While a correction factor could be calculated, this was outside the scope of this project and would require empirical research at harvest sites. This study was more concerned with the large-scale processes of decay.

Additionally, the macro climate data comes from 2007 – 2017 when California experienced a severe and sustained drought. This was a hot drought when temperatures were above average, and precipitation was below average. These conditions affect decay differently as increasing temperatures will increase the decay rate, only if there is sufficient moisture. Areas that are already relatively dry will have slower decay rates as the lack of precipitation inhibits decay.

While this method skews the climate data it may be more representative of future climate conditions in California. With climate change, California is expected to be hotter and drier. Since decay is being modeled out into the future using climate data that is more representative of future conditions may help to model decay better.

Climate Modifier Values

The climate modifier values are the product of two climate equations and long-term weather data. This approach could be extended to include projected temperature and precipitation conditions to examine how climate change may affect decomposition in the future.

As shown in the residence time rasters (Figure 10), the area in the north-eastern Central Valley has some of shortest residence time values. This is partly due to the large concentration of oaks, which have a higher decay rate than other species. This area is also generally warm and has enough moisture to facilitate decay.

The mean decay value for Quercus is 15.3% from published studies, which is less than the maximum values of the CWD decay values (16.8%) and FWD decay values (27.9%). The maximum calculated decay rates are higher than most reported values, which is a product of the climate modifier. The calculated decay rates are not as high as some values reported in Australian species of 33% and 41% for Eucalyptus (S. Brown et al., 1996).

There are concerns with using a constant $Q10$ as this factor can vary significantly at high and low temperatures (Wang, Bond-Lamberty, & Gower, 2002). When testing this function on LIDET data, it was found to perform the worst in areas with extreme temperatures, although it outperformed other temperature equations (Adair et al., 2008a).

REFERENCES OR LITERATURE CITED

Abatzoglou, J. T. (2013). Development of gridded surface meteorological data for ecological applications and modelling. *International Journal of Climatology*, *33*(1), 121–131. https://doi.org/10.1002/joc.3413

Adair, E. C., Parton, W. J., Del Grosso, S. J., Silver, W. L., Harmon, M. E., Hall, S. A., Burke, I. C., & Hart, S. C. (2008a). Simple three-pool model accurately describes patterns of long-term litter decomposition in diverse climates. *Global Change Biology*. https://doi.org/10.1111/j.1365-2486.2008.01674.x

Adair, E. C., Parton, W. J., Del Grosso, S. J., Silver, W. L., Harmon, M. E., Hall, S. A., Burke, I. C., & Hart, S. C. (2008b). Simple three-pool model accurately describes patterns of long-term litter decomposition in diverse climates. *Global Change Biology*. https://doi.org/10.1111/j.1365-2486.2008.01674.x

Barber, B. L., & Van Lear, D. H. (1984). Weight Loss and Nutrient Dynamics in Decomposing Woody Loblolly Pine Logging Slash. *Soil Science Society of America Journal*, *48*(4), 906–910. https://doi.org/10.2136/sssaj1984.03615995004800040041x

Berndes, G., Abt, B., & Asikainen, A. (2016). *Forest biomass, carbon neutrality and climate change mitigation*. EFI.

Biomass Technology Group. (2002). *Methane and nitrous oxide emissions from biomass waste stockpiles* (No. 12; p. 94). World Bank. https://wbcarbonfinance.org/docs/CH4_emissions_from_woodwaste_stockpiles.pdf

Bradshaw, L. S., Deeming, J. E., Burgan, R. E., & Cohen, J. D. (1984). *The 1978 National Fire-Danger Rating System: Technical documentation* (INT-GTR-169; p. INT-GTR-169). U.S. Department of Agriculture, Forest Service, Intermountain Forest and Range Experiment Station. https://doi.org/10.2737/INT-GTR-169

Brown, J. K., Marsden, M. A., Ryan, K. C., & Reinhardt, E. D. (1985). *Predicting duff and woody fuel consumed by prescribed fire in the Northern Rocky Mountains* (INT-RP-337). U.S. Department of Agriculture, Forest Service, Intermountain Forest and Range Experiment Station. https://doi.org/10.2737/INT-RP-337

Brown, S., Mo, J., McPherson, J. K., & Bell, D. T. (1996). Decomposition of woody debris in Western Australian forests. *Canadian Journal of Forest Research*, *26*(6), 954–966. https://doi.org/10.1139/x26-105

Comnick, J. M., & Rodgers, L. (2018). Methods to Develop the Forestland Database for the California Biopower Impacts Project. *Precision Forestry Cooperative*, 17.

Cornwell, W. K., Cornelissen, J. H. C., Amatangelo, K., Dorrepaal, E., Eviner, V. T., Godoy, O., Hobbie, S. E., Hoorens, B., Kurokawa, H., Pérez-Harguindeguy, N., Quested, H. M., Santiago, L. S., Wardle, D. A., Wright, I. J., Aerts, R., Allison, S. D., van Bodegom, P., Brovkin, V., Chatain, A., Westoby, M. (2008). Plant species traits are the predominant control on litter decomposition rates within biomes worldwide. *Ecology Letters*, *11*(10), 1065–1071. https://doi.org/10.1111/j.1461-0248.2008.01219.x

Dore, S., Fry, D. L., Collins, B. M., Vargas, R., York, R. A., & Stephens, S. L. (2016). Management Impacts on Carbon Dynamics in a Sierra Nevada Mixed Conifer Forest. *PLOS ONE*, *11*(2), e0150256. https://doi.org/10.1371/journal.pone.0150256

Eaton, J. M., & Lawrence, D. (2006). Woody debris stocks and fluxes during succession in a dry tropical forest. *Forest Ecology and Management*, *232*(1), 46–55. https://doi.org/10.1016/j.foreco.2006.05.038

Edmonds, R. L., Vogt, D. J., Sandberg, D. H., & Driver, C. H. (1986). Decomposition of Douglas-fir and red alder wood in clear-cuttings. *Canadian Journal of Forest Research*, *16*(4), 822–831. https://doi.org/10.1139/x86-145

EPA. (2014). *Framework for Assessing Biogenic CO2 Emissions from Stationary Sources*. United States Environmental Protection Agency, Office of Air and Radiation.

Erickson, H. E., Edmonds, R. L., & Peterson, C. E. (1985). Decomposition of logging residues in Douglas-fir, western hemlock, Pacific silver fir, and ponderosa pine ecosystems. *Canadian Journal of Forest Research*, *15*(5), 914–921. https://doi.org/10.1139/x85-147

Estes, B. L., Knapp, E. E., Skinner, C. N., & Uzoh, F. C. C. (2012). Seasonal variation in surface fuel moisture between unthinned and thinned mixed conifer forest, northern California, USA. *International Journal of Wildland Fire*, *21*(4), 428. https://doi.org/10.1071/WF11056

Finér, L., Jurgensen, M., Palviainen, M., Piirainen, S., & Page-Dumroese, D. (2016). Does clear-cut harvesting accelerate initial wood decomposition? A five-year study with standard wood material. *Forest Ecology and Management*, *372*, 10–18. https://doi.org/10.1016/j.foreco.2016.03.060

Follett, R. F., Kimble, J. M., & Lal, R. (Eds.). (2001). *The potential of US grazing lands to sequester carbon and mitigate the greenhouse effect*. Lewis.

Gholz, H. L., Wedin, D. A., Smitherman, S. M., Harmon, M. E., & Parton, W. J. (2000). Long-term dynamics of pine and hardwood litter in contrasting environments:

Toward a global model of decomposition. *Global Change Biology*, *6*(7), 751–765. https://doi.org/10.1046/j.1365-2486.2000.00349.x

Giuntoli, J., Caserini, S., Marelli, L., Baxter, D., & Agostini, A. (2015). Domestic heating from forest logging residues: Environmental risks and benefits. *Journal of Cleaner Production*, *99*, 206–216. https://doi.org/10.1016/j.jclepro.2015.03.025

Hardy, C. C. (1996). *Guidelines for Estimating Volume, Biomass, and Smoke*.

Hardy, C. C. (1999). *Procedures for estimating pile volume, biomass, emissions*.

Harmon, M. E., Franklin, J. F., Swanson, F. J., Sollins, P., Gregory, S. V., Lattin, J. D., Anderson, N. H., Cline, S. P., Aumen, N. G., Sedell, J. R., Lienkaemper, G. W., Cromack, K., & Cummins, K. W. (1986). Ecology of Coarse Woody Debris in Temperate Ecosystems. In A. MacFadyen & E. D. Ford (Eds.), *Advances in Ecological Research* (Vol. 15, pp. 133–302). Academic Press. https://doi.org/10.1016/S0065-2504(08)60121-X

Harmon, M. E., Krankina, O. N., & Sexton, J. (2000). Decomposition vectors: A new approach to estimating woody detritus decomposition dynamics. *Canadian Journal of Forest Research*, *30*(1), 76–84.

Hille, M. G., & Stephens, S. L. (2005). Mixed Conifer Forest Duff Consumption during Prescribed Fires: Tree Crown Impacts. *Forest Science*, *51*(5), 8.

Intergovernmental Panel on Climate Change. (2014). *Climate Change 2014 Mitigation of Climate Change: Working Group III Contribution to the Fifth Assessment Report of the Intergovernmental Panel on Climate Change*. Cambridge University Press. https://doi.org/10.1017/CBO9781107415416

Johnson, E. A., & Greene, D. F. (1991). A method for studying dead bole dynamics in Pinus contorta var. Latifolia—Picea engelmannii forests. *Journal of Vegetation Science*, *2*(4), 523–530. https://doi.org/10.2307/3236034

Kahl, T., Arnstadt, T., Baber, K., Bässler, C., Bauhus, J., Borken, W., Buscot, F., Floren, A., Heibl, C., Hessenmöller, D., Hofrichter, M., Hoppe, B., Kellner, H., Krüger, D., Linsenmair, K. E., Matzner, E., Otto, P., Purahong, W., Seilwinder, C., … Gossner, M. M. (2017). Wood decay rates of 13 temperate tree species in relation to wood properties, enzyme activities and organismic diversities. *Forest Ecology and Management*, *391*, 86–95. https://doi.org/10.1016/j.foreco.2017.02.012

Laiho, R., & Prescott, C. E. (2004). Decay and nutrient dynamics of coarse woody debris in northern coniferous forests: A synthesis. *Canadian Journal of Forest Research*, *34*(4), 763–777. https://doi.org/10.1139/x03-241

Laird, J., & Pimlott, K. (2018). *California Forest Practice Rules 2018* (p. 420) [Rules and Regulations]. CAL FIRE.

LIDET. (1995). Meeting the Challenge of Long-Term, Broad-Scale Ecological Experiments. *LTER Nework*, *19*, 32.

Lloyd, J., & Taylor, J. A. (1994). On the temperature dependence of soil respiration. *Functional Ecology*, 315–323.

Mackensen, J., & Bauhus, J. (1999). *The Decay of Coarse Woody Debris* (National Carbon Accounting System Technical Report No. 6; p. 51).

MacMillan, P. C. (1988). Decomposition of coarse woody debris in an old-growth Indiana forest. *Canadian Journal of Forest Research*, *18*(11), 1353–1362. https://doi.org/10.1139/x88-212

Mann, M., & Spath, P. (2001). A life cycle assessment of biomass cofiring in a coal-fired power plant. *Clean Products and Processes*, *3*(2), 81–91. https://doi.org/10.1007/s100980100109

Mattson, K. (1987). Decomposition of woody debris in a regenerating, clear-cut forest in the Southern Appalachians—Canadian Journal of Forest Research. *Canadian Journal of Forest Research*, *17*, 10.

McColl, J. G., & Powers, R. F. (2003). Decomposition of small woody debris of California red fir: Mass loss and elemental content over 17 years. *Soil Science Society of America Journal; Madison*, *67*(4), 1227.

Melin, Y., Petersson, H., & Nordfjell, T. (2009). Decomposition of stump and root systems of Norway spruce in Sweden—A modelling approach. *Forest Ecology and Management*, *257*(5), 1445–1451. https://doi.org/10.1016/j.foreco.2008.12.020

Miller, C., & Boston, K. (2017). The Quantification of Logging Residues in Oregon with Impacts on Sustainability and Availability of Raw Material for Future Biomass Energy. *European Journal of Forest Engineering*, *3*(1), 16–22.

Müller-Using, S., & Bartsch, N. (2009). Decay dynamic of coarse and fine woody debris of a beech (Fagus sylvatica L.) forest in Central Germany. *European Journal of Forest Research*, *128*(3), 287–296. https://doi.org/10.1007/s10342-009-0264-8

Næsset, E. (1999). Decomposition rate constants of Picea abies logs in southeastern Norway. *Canadian Journal of Forest Research*, *29*(3), 372–381.

Ohmann, J. L., & Gregory, M. J. (2002). Predictive mapping of forest composition and structure with direct gradient analysis and nearest- neighbor imputation in coastal Oregon, U.S.A. *Canadian Journal of Forest Research*, *32*(4), 725–741. https://doi.org/10.1139/x02-011

Olson, J. S. (1963). Energy Storage and the Balance of Producers and Decomposers in Ecological Systems. *Ecology*, *44*(2), 322–331. https://doi.org/10.2307/1932179

Pierobon, F., Ganguly, I., Anfodillo, T., & Eastin, I. L. (2014). Evaluation of environmental impacts of harvest residue-based bioenergy using radiative forcing analysis. *The Forestry Chronicle*, *90*(5), 577–585.

Pietsch, K. A., Ogle, K., Cornelissen, J. H. C., Cornwell, W. K., Bönisch, G., Craine, J. M., Jackson, B. G., Kattge, J., Peltzer, D. A., Penuelas, J., Reich, P. B., Wardle, D. A., Weedon, J. T., Wright, I. J., Zanne, A. E., & Wirth, C. (2014). Global relationship of wood and leaf litter decomposability: The role of functional traits within and across plant organs: Global relationship of wood and leaf litter decomposability. *Global Ecology and Biogeography*, *23*(9), 1046–1057. https://doi.org/10.1111/geb.12172

Powers, R. F., Andrew Scott, D., Sanchez, F. G., Voldseth, R. A., Page-Dumroese, D., Elioff, J. D., & Stone, D. M. (2005). The North American long-term soil productivity experiment: Findings from the first decade of research. *Forest Ecology and Management*, *220*(1–3), 31–50. https://doi.org/10.1016/j.foreco.2005.08.003

Rebain, S., Reinhardt, E., Crookston, N., & Beukema, S. (2015). *The Fire and Fuels Extension to the Forest Vegetation Simulator: Updated Model Documentation*. 411.

Risch, A. C., Jurgensen, M. F., Page-Dumroese, D. S., & Schütz, M. (2013). Initial turnover rates of two standard wood substrates following land-use change in subalpine ecosystems in the Swiss Alps. *Canadian Journal of Forest Research*, *43*(10), 901–910. https://doi.org/10.1139/cjfr-2013-0109

Sierra, C. A., Müller, M., & Trumbore, S. E. (2012). Models of soil organic matter decomposition: The SoilR package, version 1.0. *Geosci. Model Dev.*, *5*(4), 1045–1060. https://doi.org/10.5194/gmd-5-1045-2012

Sierra Carlos A., Trumbore Susan E., Davidson Eric A., Vicca Sara, & Janssens I. (2015). Sensitivity of decomposition rates of soil organic matter with respect to simultaneous changes in temperature and moisture. *Journal of Advances in Modeling Earth Systems*, *7*(1), 335–356. https://doi.org/10.1002/2014MS000358

Smith, A. C., Bhatti, J. S., Chen, H., Harmon, M. E., & Arp, P. A. (2011). Modelling above- and below-ground mass loss and N dynamics in wooden dowels (LIDET) placed across North and Central America biomes at the decadal time scale. *Ecological Modelling*, *222*(14), 2276–2290. https://doi.org/10.1016/j.ecolmodel.2010.09.018

Swift, M. J., Healey, I. N., Hibberd, J. K., Sykes, J. M., Bampoe, V., & Nesbitt, M. E. (1976). The decomposition of branch-wood in the canopy and floor of a mixed deciduous woodland. *Oecologia*, *26*(2), 139–149. https://doi.org/10.1007/BF00582892

Tuomi, M., Thum, T., Järvinen, H., Fronzek, S., Berg, B., Harmon, M., Trofymow, J. A., Sevanto, S., & Liski, J. (2009). Leaf litter decomposition—Estimates of global variability based on Yasso07 model. *ArXiv:0906.0886 [q-Bio]*. http://arxiv.org/abs/0906.0886

Urbanski, S. (2014). Wildland fire emissions, carbon, and climate: Emission factors. *Forest Ecology and Management*, *317*, 51–60. https://doi.org/10.1016/j.foreco.2013.05.045

Wagener, W. W., & Offord, H. R. (1972). *Logging slash: Its breakdown and decay at two forests in northern California*.

Weedon, J. T., Cornwell, W. K., Cornelissen, J. H. C., Zanne, A. E., Wirth, C., & Coomes, D. A. (2009). Global meta-analysis of wood decomposition rates: A role for trait variation among tree species? *Ecology Letters*, *12*(1), 45–56. https://doi.org/10.1111/j.1461-0248.2008.01259.x

Winterbourne, A. H. S. (2016). *Slash-pile biomass estimations and Carbon- Cycling in the Coastal Temperate Rainforest of the Pacific Northwest* [Master's Case Study]. Oregon State University.

Woodall, C. W., & Liknes, G. C. (2008). Relationships between forest fine and coarse woody debris carbon stocks across latitudinal gradients in the United States as an indicator of climate change effects. *Ecological Indicators*, *8*(5), 686–690. https://doi.org/10.1016/j.ecolind.2007.11.002

Woodall, C. W., & Williams, M. S. (2005). Sampling, Estimation, and Analysis Procedures for the Down Woody Materials Indicator. *USDA Forest Service, General Technical Report*.

Wright, C. S., Evans, A. M., & Restaino, J. (2017). *Decomposition Rates for Hand-piled Fuels*. United States Department of Agriculture, Forest Service, Pacific Northwest Research Station.

Yin, X. (1999). The decay of forest woody debris: Numerical modeling and implications based on some 300 data cases from North America. *Oecologia*, *121*(1), 81–98. https://doi.org/10.1007/s004420050909

Zell, J., Kändler, G., & Hanewinkel, M. (2009). Predicting constant decay rates of coarse woody debris—A meta-analysis approach with a mixed model. *Ecological Modelling*, *220*(7), 904–912. https://doi.org/10.1016/j.ecolmodel.2009.01.020

APPENDIX A

Appendix A: All Decay Values

full_name	classification	size_class_cm	k_const	climate_normalized_k	ref
Abies amabilis	Gymnosperm	1.5	0.002	0.012007	Erickson et al. 1985
Abies amabilis	Gymnosperm	10	0.009	0.054031	Erickson et al. 1985
Abies amabilis	Gymnosperm	1.5	0.003	0.01801	Erickson et al. 1985
Abies amabilis	Gymnosperm	10	0.009	0.054031	Erickson et al. 1985
Abies amabilis	Gymnosperm	52	0.051	0.051	Harmon 2005
Abies balsamea	Gymnosperm	12.5	0.033	0.068863	Foster & Lang 1982
Abies balsamea	Gymnosperm	12.5	0.038	0.079297	Foster & Lang 1982
Abies balsamea	Gymnosperm	8	0.0299	0.065654	Lambert et al. 1980
Abies concolor	Gymnosperm	20	0.049	0.075672	Harmon 1987
Abies concolor	Gymnosperm	branch	0.049	0.075672	Harmon 1987
Abies concolor	Gymnosperm	bark	0.027	0.041697	Harmon 1987
Abies concolor	Gymnosperm	52	0.035	0.057804	Harmon 2005
Abies concolor	Gymnosperm	52	0.051	0.065583	Harmon 2005
Abies concolor	Gymnosperm	litter	0.13	0.165889	Stohlgren 1988
Abies concolor	Gymnosperm	litter	0.14	0.17865	Stohlgren 1988
Abies grandis	Gymnosperm	52	0.038	0.053344	Harmon 2005
Abies lasiocarpa	Gymnosperm	52	0.035	0.106399	Harmon 2005
Abies lasiocarpa	Gymnosperm	foliage	0.149	0.238153	Keane et al. 2008
Abies lasiocarpa	Gymnosperm	twigs (1hr)	0.113	0.180613	Keane et al. 2008
Abies lasiocarpa	Gymnosperm	large branch (100hr)	0.053	0.084712	Keane et al. 2008
Abies lasiocarpa	Gymnosperm	branch	0.0353	0.066495	Taylor et al. 1991

full_name	classification	size_class_cm	k_const	climate_normalized_k	ref
Abies lasiocarpa	Gymnosperm	twigs (1hr)	0.062	0.116789	Taylor et al. 1991
Abies lasiocarpa	Gymnosperm	needles	0.0933	0.175749	Taylor et al. 1991
Abies magnifica	Gymnosperm	52	0.043	0.071016	Harmon 2005
Abies procera	Gymnosperm	52	0.03	0.035676	Harmon 2005
Abies spp.	Gymnosperm	log	0.072	0.082066	Janish 2005
Abies spp.	Gymnosperm	bark	0.004	0.004559	Janish 2005
Abies spp.	Gymnosperm	8	0.032	0.095196	Shorohova and Kapitsa
Acer rubrum	Angiosperm	10	0.08	0.081597	Harmon 1982
Acer rubrum	Angiosperm	14.5	0.081	0.06345	Mattson 1987
Acer spp.	Angiosperm	31	0.053	0.070017	Kahl et al. 2017
Acer spp.	Angiosperm	18	0.0452	0.038264	MacMillan 1988
Alnus rubra	Angiosperm	1.5	0.23	0.237491	Edmonds et al. 1986
Alnus rubra	Angiosperm	5	0.122	0.125974	Edmonds et al. 1986
Alnus rubra	Angiosperm	10	0.088	0.090866	Edmonds et al. 1986
Alnus rubra	Angiosperm	1.5	0.115	0.118746	Edmonds et al. 1986
Alnus rubra	Angiosperm	5	0.109	0.11255	Edmonds et al. 1986
Alnus rubra	Angiosperm	10	0.04	0.041303	Edmonds et al. 1986
Alnus rubra	Angiosperm	1.5	0.146	0.150755	Edmonds et al. 1986
Alnus rubra	Angiosperm	5	0.086	0.088801	Edmonds et al. 1986
Alnus rubra	Angiosperm	10	0.119	0.122876	Edmonds et al. 1986
Alnus rubra	Angiosperm	1.5	0.145	0.149723	Edmonds et al. 1986
Alnus rubra	Angiosperm	5	0.093	0.096029	Edmonds et al. 1986
Alnus rubra	Angiosperm	10	0.035	0.03614	Edmonds et al. 1986
Alnus rubra	Angiosperm	25	0.083	0.083	Harmon 2005
Alnus rubra	Angiosperm	25	0.055	0.055	Harmon 2005
Betula costata	Angiosperm	log	0.03	0.132549	Yatskov et al. 2003

full_name	classification	size_class_cm	k_const	climate_normalized_k	ref
Betula costata	Angiosperm	snag	0.081	0.357881	Yatskov et al. 2003
Betula lenta	Angiosperm	21.5	0.149	0.116716	Mattson 1987
Betula pendula	Angiosperm	logs	0.046	0.089081	Harmon 2000
Betula pendula	Angiosperm	log	0.054	0.112708	Yatskov et al. 2003
Betula pendula	Angiosperm	log	0.061	0.367268	Yatskov et al. 2003
Betula pendula	Angiosperm	log	0.042	0.37652	Yatskov et al. 2003
Betula pendula	Angiosperm	log	0.078	0.344626	Yatskov et al. 2003
Betula pendula	Angiosperm	snag	0.027	0.056354	Yatskov et al. 2003
Betula pendula	Angiosperm	snag	0.056	0.337164	Yatskov et al. 2003
Betula pendula	Angiosperm	snag	0.052	0.466168	Yatskov et al. 2003
Betula pendula	Angiosperm	snag	0.088	0.388809	Yatskov et al. 2003
Betula spp.	Angiosperm	31	0.042	0.055485	Kahl et al. 2017
Betula spp.	Angiosperm	log	0.045	0.078174	Krankina & Harmon 1995
Betula spp.	Angiosperm	8	0.066	0.196341	Shorohova and Kapitsa
Betula spp.	Angiosperm	10	0.088	0.170457	Tarasov and Birdsey 2001
Betula spp.	Angiosperm	37.5	0.039	0.075543	Tarasov and Birdsey 2001
Betula spp.	Angiosperm	bark	0.023	0.044551	Tarasov and Birdsey 2001
Calocedrus decurrens	Gymnosperm	52	0.02	0.024599	Harmon 2005
Calocedrus decurrens	Gymnosperm	litter	0.16	0.204171	Stohlgren 1988
Carya spp.	Angiosperm	10	0.08	0.081597	Harmon 1982
Carya spp.	Angiosperm	29.66667	0.035	0.029629	MacMillan 1988

full_name	classification	size_class_cm	k_const	climate_normalized_k	ref
Carya spp.	Angiosperm	13	0.166	0.130033	Mattson 1987
Cornus florida	Angiosperm	10	0.05	0.050998	Harmon 1982
Cornus florida	Angiosperm	6.3	0.125	0.097916	Mattson 1987
Eucalyptus calophylla	Angiosperm	bole and branch	0.215	0.155677	Brown et al. 1996
Eucalyptus calophylla	Angiosperm	4	0.407949	0.295388	Brown et al. 1996
Eucalyptus calophylla	Angiosperm	12.5	0.113311	0.082046	Brown et al. 1996
Eucalyptus diversicolor	Angiosperm	bole and branch	0.174	0.12599	Brown et al. 1996
Eucalyptus diversicolor	Angiosperm	4	0.330154	0.239058	Brown et al. 1996
Eucalyptus diversicolor	Angiosperm	12.5	0.091703	0.0664	Brown et al. 1996
Eucalyptus diversicolor	Angiosperm	0.8	0.107	0.06686	O'connell 1997
Eucalyptus diversicolor	Angiosperm	1.1	0.12	0.074983	O'connell 1997
Eucalyptus diversicolor	Angiosperm	1.4	0.094	0.058737	O'connell 1997
Eucalyptus diversicolor	Angiosperm	2.5	0.046	0.028743	O'connell 1997
Eucalyptus diversicolor	Angiosperm	4.3	0.03	0.018746	O'connell 1997
Eucalyptus diversicolor	Angiosperm	8.4	0.022	0.013747	O'connell 1997
Eucalyptus maculata	Angiosperm	20	0.049	0.028539	Mackensen and Bauhus 2003

full_name	classification	size_class_cm	k_const	climate_normalized_k	ref
Eucalyptus marginata	Angiosperm	bole and branch	0.067	0.048513	Brown et al. 1996
Eucalyptus marginata	Angiosperm	4	0.127128	0.092051	Brown et al. 1996
Eucalyptus marginata	Angiosperm	12.5	0.035311	0.025568	Brown et al. 1996
Eucalyptus regnans	Angiosperm	20	0.041	0.029663	Mackensen and Bauhus 2003
Fraxinus profunda	Angiosperm	13.75	0.071	0.030876	Rice et al. 1997
Fraxinus profunda	Angiosperm	1.5	0.071	0.030876	Rice et al. 1997
Fraxinus spp.	Angiosperm	31	0.019	0.0251	Kahl et al. 2017
Juniperus communis	Gymnosperm	7.5	0.008	0.009076	Devries and Kuyper 1988
Juniperus communis	Gymnosperm	7.5	0.027	0.030633	Devries and Kuyper 1988
Juniperus communis	Gymnosperm	7.5	0.044	0.049921	Devries and Kuyper 1988
Juniperus communis	Gymnosperm	7.5	0.025	0.028364	Devries and Kuyper 1988
Juniperus communis	Gymnosperm	7.5	0.06	0.068075	Devries and Kuyper 1988
Juniperus communis	Gymnosperm	7.5	0.055	0.062403	Devries and Kuyper 1988
Juniperus occidentalis	Gymnosperm	litter	0.16	0.498682	Bates et al. 2007
Juniperus occidentalis	Gymnosperm	litter	0.09	0.280508	Bates et al. 2007
Larix dahurica	Gymnosperm	log	0.015	0.090312	Yatskov et al. 2003
Larix dahurica	Gymnosperm	snag	0.009	0.054187	Yatskov et al. 2003
Larix siberica	Gymnosperm	log	0.023	0.138478	Yatskov et al. 2003

full_name	classification	size_class_cm	k_const	climate_normalized_k	ref
Larix siberica	Gymnosperm	log	0.031	0.277908	Yatskov et al. 2003
Larix siberica	Gymnosperm	snag	0.004	0.024083	Yatskov et al. 2003
Larix siberica	Gymnosperm	snag	0.01	0.089648	Yatskov et al. 2003
Larix spp.	Gymnosperm	31	0.004	0.005284	Kahl et al. 2017
Picea abies	Gymnosperm	logs	0.033	0.063906	Harmon 2000
Picea abies	Gymnosperm	10	0.0275	0.054719	Naesset 1999
Picea abies	Gymnosperm	12.5	0.0342	0.068051	Naesset 1999
Picea abies	Gymnosperm	18	0.0435	0.086556	Naesset 1999
Picea abies	Gymnosperm	23	0.0391	0.077801	Naesset 1999
Picea abies	Gymnosperm	25	0.0412	0.08198	Naesset 1999
Picea abies	Gymnosperm	12.5	0.059	0.114284	Tarasov and Birdsey 2001
Picea abies	Gymnosperm	30	0.022	0.042614	Tarasov and Birdsey 2001
Picea abies	Gymnosperm	50	0.0215	0.041646	Tarasov and Birdsey 2001
Picea abies	Gymnosperm	bark	0.017	0.032929	Tarasov and Birdsey 2001
Picea abies	Gymnosperm	coarse roots	0.027	0.052299	Tarasov and Birdsey 2001
Picea abies	Gymnosperm	log	0.026	0.054267	Yatskov et al. 2003
Picea abies	Gymnosperm	snag	0.044	0.091836	Yatskov et al. 2003
Picea ajanensis	Gymnosperm	log	0.028	0.123712	Yatskov et al. 2003
Picea ajanensis	Gymnosperm	snag	0.035	0.15464	Yatskov et al. 2003
Picea engelmannii	Gymnosperm	52	0.028	0.085119	Harmon 2005
Picea engelmannii	Gymnosperm	10	0.0054	0.013419	Johnson and Green 1991

full_name	classification	size_class_cm	k_const	climate_normalized_k	ref
Picea engelmannii	Gymnosperm	10	0.0025	0.006212	Johnson and Green 1991
Picea engelmannii	Gymnosperm	15.6	0.0013	0.006693	Kueppers et al. 2004
Picea engelmannii	Gymnosperm	15.6	0.0015	0.007723	Kueppers et al. 2004
Picea engelmannii	Gymnosperm	branch	0.0265	0.049918	Taylor et al. 1991
Picea engelmannii	Gymnosperm	twigs (1hr)	0.0549	0.103415	Taylor et al. 1991
Picea engelmannii	Gymnosperm	needles	0.1828	0.34434	Taylor et al. 1991
Picea glauca	Gymnosperm	12.7	0.071	0.139418	Alban and Pastor 1993
Picea obovata	Gymnosperm	log	0.049	0.295019	Yatskov et al. 2003
Picea obovata	Gymnosperm	snag	-6.00E-04	-0.00361	Yatskov et al. 2003
Picea rubens	Gymnosperm	12.5	0.033	0.068863	Foster & Lang 1982
Picea rubens	Gymnosperm	20	0.027	0.056343	Foster & Lang 1982
Picea rubens	Gymnosperm	25	0.032	0.066776	Foster & Lang 1982
Picea rubens	Gymnosperm	12.5	0.011	0.022954	Foster & Lang 1982
Picea rubens	Gymnosperm	20	0.014	0.029215	Foster & Lang 1982
Picea rubens	Gymnosperm	25	0.022	0.045909	Foster & Lang 1982
Picea sitchensis	Gymnosperm	>60	0.0096	0.010611	Graham and Cromack 1982
Picea sitchensis	Gymnosperm	<60	0.0119	0.013153	Graham and Cromack 1982
Picea sitchensis	Gymnosperm	all	0.0111	0.012269	Graham and Cromack 1982
Picea sitchensis	Gymnosperm	52	0.023	0.023	Harmon 2005
Picea spp.	Gymnosperm	31	0.035	0.046238	Kahl et al. 2017
Picea spp.	Gymnosperm	log	0.034	0.059065	Krankina & Harmon 1995

full_name	classification	size_class_cm	k_const	climate_normalized_k	ref
Pinus albicaulis	Gymnosperm	foliage	0.169	0.27012	Keane et al. 2008
Pinus albicaulis	Gymnosperm	twigs (1hr)	0.068	0.108687	Keane et al. 2008
Pinus albicaulis	Gymnosperm	branch (10hr)	0.083	0.132662	Keane et al. 2008
Pinus albicaulis	Gymnosperm	large branch (100hr)	0.061	0.097499	Keane et al. 2008
Pinus banksiana	Gymnosperm	14.4	0.042	0.082472	Alban and Pastor 1993
Pinus contorta	Gymnosperm	25	0.027	0.027165	Busse 1994
Pinus contorta	Gymnosperm	15	0.0163	0.050254	Fahey 1983
Pinus contorta	Gymnosperm	52	0.042	0.060801	Harmon 2005
Pinus contorta	Gymnosperm	52	0.023	0.069919	Harmon 2005
Pinus contorta	Gymnosperm	10	0.0171	0.042493	Johnson and Green 1991
Pinus contorta	Gymnosperm	10	0.0299	0.0743	Johnson and Green 1991
Pinus contorta	Gymnosperm	10	0.0153	0.03802	Johnson and Green 1991
Pinus contorta	Gymnosperm	10	0.0045	0.011182	Johnson and Green 1991
Pinus contorta	Gymnosperm	10	0.0035	0.008697	Johnson and Green 1991
Pinus contorta	Gymnosperm	branch	0.0521	0.098141	Taylor et al. 1991
Pinus contorta	Gymnosperm	twigs (1hr)	0.0549	0.103415	Taylor et al. 1991
Pinus contorta	Gymnosperm	needles	0.1151	0.216814	Taylor et al. 1991
Pinus contorta	Gymnosperm	litter	0.235	0.541127	Yavitt and Fahey 1986
Pinus jefferyi	Gymnosperm	52	0.042	0.05401	Harmon 2005
Pinus koraiensis	Gymnosperm	log	0.015	0.066274	Yatskov et al. 2003
Pinus koraiensis	Gymnosperm	snag	0.003	0.013255	Yatskov et al. 2003

full_name	classification	size_class_cm	k_const	climate_normalized_k	ref
Pinus lambertiana	Gymnosperm	52	0.036	0.046294	Harmon 2005
Pinus lambertiana	Gymnosperm	litter	0.12	0.153128	Stohlgren 1988
Pinus lambertiana	Gymnosperm	litter	0.1	0.127607	Stohlgren 1988
Pinus monticola	Gymnosperm	52	0.035	0.049133	Harmon 2005
Pinus nigra	Gymnosperm	litter	0.17	0.191141	Moro and Domingo 2000
Pinus pinaster	Gymnosperm	bole and branch	0.049	0.03548	Brown et al. 1996
Pinus pinaster	Gymnosperm	4	0.092974	0.067321	Brown et al. 1996
Pinus pinaster	Gymnosperm	12.5	0.025824	0.018699	Brown et al. 1996
Pinus pinaster	Gymnosperm	litter	0.12	0.134923	Moro and Domingo 2000
Pinus ponderosa	Gymnosperm	10	0.013	0.01737	Erickson et al. 1985
Pinus ponderosa	Gymnosperm	10	0.012	0.016034	Erickson et al. 1985
Pinus ponderosa	Gymnosperm	1.5	0.005	0.006681	Erickson et al. 1985
Pinus ponderosa	Gymnosperm	1.5	0.009	0.012025	Erickson et al. 1985
Pinus ponderosa	Gymnosperm	52	0.011	0.015442	Harmon 2005
Pinus ponderosa	Gymnosperm	litter	0.37	0.254345	Hart et al. 1992
Pinus ponderosa	Gymnosperm	litter	0.17	0.116861	Hart et al. 1992
Pinus ponderosa	Gymnosperm	litter	0.19	0.130609	Hart et al. 1992
Pinus ponderosa	Gymnosperm	litter	0.08	0.054993	Hart et al. 1992
Pinus ponderosa	Gymnosperm	15.6	0.0029	0.014932	Kueppers et al. 2004
Pinus ponderosa	Gymnosperm	15.6	0.0016	0.008238	Kueppers et al. 2004
Pinus radiata	Gymnosperm	20	0.127	0.096147	Mackensen and Bauhus 2003
Pinus resinosa	Gymnosperm	14.4	0.055	0.107999	Alban and Pastor 1993
Pinus rigida	Gymnosperm	10	0.06	0.061198	Harmon 1982

full_name	classification	size_class_cm	k_const	climate_normalized_k	ref
Pinus rigida	Gymnosperm	6.9	0.063	0.04935	Mattson 1987
Pinus siberica	Gymnosperm	log	0.019	0.170331	Yatskov et al. 2003
Pinus siberica	Gymnosperm	snag	0.003	0.026894	Yatskov et al. 2003
Pinus sibirica	Gymnosperm	8	0.014	0.041648	Shorohova and Kapitsa
Pinus spp.	Gymnosperm	31	0.016	0.021137	Kahl et al. 2017
Pinus spp.	Gymnosperm	log	0.033	0.057328	Krankina & Harmon 1995
Pinus sylvestris	Gymnosperm	7.5	0.022	0.024963	Devries and Kuyper 1988
Pinus sylvestris	Gymnosperm	7.5	0.134	0.152049	Devries and Kuyper 1988
Pinus sylvestris	Gymnosperm	7.5	0.054	0.061274	Devries and Kuyper 1988
Pinus sylvestris	Gymnosperm	7.5	0.042	0.047658	Devries and Kuyper 1988
Pinus sylvestris	Gymnosperm	7.5	0.113	0.128225	Devries and Kuyper 1988
Pinus sylvestris	Gymnosperm	7.5	0.109	0.123688	Devries and Kuyper 1988
Pinus sylvestris	Gymnosperm	logs	0.035	0.067779	Harmon 2000
Pinus sylvestris	Gymnosperm	8	0.027	0.080321	Shorohova and Kapitsa
Pinus sylvestris	Gymnosperm	10	0.041	0.079417	Tarasov and Birdsey 2001
Pinus sylvestris	Gymnosperm	25	0.0185	0.035835	Tarasov and Birdsey 2001
Pinus sylvestris	Gymnosperm	45	0.018	0.034866	Tarasov and Birdsey 2001

full_name	classification	size_class_cm	k_const	climate_normalized_k	ref
Pinus sylvestris	Gymnosperm	bark	0.009	0.017433	Tarasov and Birdsey 2001
Pinus sylvestris	Gymnosperm	log	0.027	0.056354	Yatskov et al. 2003
Pinus sylvestris	Gymnosperm	log	0.044	0.264915	Yatskov et al. 2003
Pinus sylvestris	Gymnosperm	log	0.036	0.322732	Yatskov et al. 2003
Pinus sylvestris	Gymnosperm	snag	0.037	0.077226	Yatskov et al. 2003
Pinus sylvestris	Gymnosperm	snag	-0.02	-0.12042	Yatskov et al. 2003
Pinus sylvestris	Gymnosperm	snag	0.004	0.035859	Yatskov et al. 2003
Pinus taeda	Gymnosperm	small	0.058	0.033705	Barber and Van Lear 1984
Pinus taeda	Gymnosperm	medium	0.081	0.047071	Barber and Van Lear 1984
Pinus taeda	Gymnosperm	large	0.068	0.039516	Barber and Van Lear 1984
Pinus taeda	Gymnosperm	small	0.036	0.02092	Barber and Van Lear 1984
Pinus taeda	Gymnosperm	medium	0.057	0.033124	Barber and Van Lear 1984
Pinus taeda	Gymnosperm	large	0.045	0.02615	Barber and Van Lear 1984
Pinus virginiana	Gymnosperm	10	0.04	0.040799	Harmon 1982
Populus spp.	Angiosperm	31	0.055	0.072659	Kahl et al. 2017
Populus tremula	Angiosperm	15	0.071	0.137528	Tarasov and Birdsey 2001
Populus tremula	Angiosperm	42.5	0.044	0.085228	Tarasov and Birdsey 2001
Populus tremula	Angiosperm	bark	0.018	0.034866	Tarasov and Birdsey 2001

full_name	classification	size_class_cm	k_const	climate_normalized_k	ref
Populus tremuloides	Angiosperm	15.3	0.08	0.15709	Alban and Pastor 1993
Prunus spp.	Angiosperm	31	0.031	0.040953	Kahl et al. 2017
Psuedotsuga menziesii	Gymnosperm	1.5	0.036	0.037173	Edmonds et al. 1986
Psuedotsuga menziesii	Gymnosperm	5	0.027	0.027879	Edmonds et al. 1986
Psuedotsuga menziesii	Gymnosperm	10	0.013	0.013423	Edmonds et al. 1986
Psuedotsuga menziesii	Gymnosperm	1.5	0.038	0.039238	Edmonds et al. 1986
Psuedotsuga menziesii	Gymnosperm	5	0.013	0.013423	Edmonds et al. 1986
Psuedotsuga menziesii	Gymnosperm	10	0.019	0.019619	Edmonds et al. 1986
Psuedotsuga menziesii	Gymnosperm	1.5	0.033	0.034075	Edmonds et al. 1986
Psuedotsuga menziesii	Gymnosperm	5	0.022	0.022717	Edmonds et al. 1986
Psuedotsuga menziesii	Gymnosperm	10	0.007	0.007228	Edmonds et al. 1986
Psuedotsuga menziesii	Gymnosperm	1.5	0.029	0.029945	Edmonds et al. 1986
Psuedotsuga menziesii	Gymnosperm	5	0.016	0.016521	Edmonds et al. 1986
Psuedotsuga menziesii	Gymnosperm	10	0.012	0.012391	Edmonds et al. 1986
Psuedotsuga menziesii	Gymnosperm	10	0.016	0.017364	Erickson et al. 1985
Psuedotsuga menziesii	Gymnosperm	10	0.037	0.040153	Erickson et al. 1985

full_name	classification	size_class_cm	k_const	climate_normalized_k	ref
Psuedotsuga menziesii	Gymnosperm	1.5	0.004	0.004341	Erickson et al. 1985
Psuedotsuga menziesii	Gymnosperm	1.5	0.011	0.011937	Erickson et al. 1985
Psuedotsuga menziesii	Gymnosperm	52	0.015	0.015	Harmon 2005
Psuedotsuga menziesii	Gymnosperm	52	0.014	0.015957	Harmon 2005
Psuedotsuga menziesii	Gymnosperm	log	0.016	0.018237	Janish 2005
Psuedotsuga menziesii	Gymnosperm	31	0.002	0.002642	Kahl et al. 2017
Psuedotsuga menziesii	Gymnosperm	logs	0.0063	0.009094	Means et al. 1985
Psuedotsuga menziesii	Gymnosperm	logs	0.007	0.010104	Means et al. 1985
Psuedotsuga menziesii	Gymnosperm	logs	0.01	0.012981	Sollins et al. 1987
Psuedotsuga menziesii	Gymnosperm	logs	0.022	0.022	Stone et al. 1997
Psuedotsuga menziesii	Gymnosperm	20	0.067	0.067	Stone et al. 1997
Psuedotsuga menziesii	Gymnosperm	30	0.056	0.056	Stone et al. 1997
Psuedotsuga menziesii	Gymnosperm	60	0.021	0.021	Stone et al. 1997
Psuedotsuga menziesii	Gymnosperm	80	0.012	0.012	Stone et al. 1997
Quercus alba	Angiosperm	11.4	0.063	0.04935	Mattson 1987
Quercus coccinea	Angiosperm	10	0.1	0.101997	Harmon 1982

full_name	classification	size_class_cm	k_const	climate_normalized_k	ref
Quercus coccinea	Angiosperm	14.9	0.05	0.039167	Mattson 1987
Quercus prinus	Angiosperm	0.5	0.1244	0.094023	Abbott and Crossley 1982
Quercus prinus	Angiosperm	2	0.1144	0.086465	Abbott and Crossley 1982
Quercus prinus	Angiosperm	4	0.0978	0.073918	Abbott and Crossley 1982
Quercus prinus	Angiosperm	10	0.18	0.183594	Harmon 1982
Quercus prinus	Angiosperm	8.7	0.17	0.133166	Mattson 1987
Quercus robur	Angiosperm	7.5	0.066	0.074884	Devries and Kuyper 1988
Quercus robur	Angiosperm	7.5	0.273	0.309752	Devries and Kuyper 1988
Quercus robur	Angiosperm	7.5	0.489	0.554837	Devries and Kuyper 1988
Quercus robur	Angiosperm	7.5	0.253	0.287066	Devries and Kuyper 1988
Quercus robur	Angiosperm	7.5	0.151	0.171334	Devries and Kuyper 1988
Quercus robur	Angiosperm	7.5	0.175	0.198568	Devries and Kuyper 1988
Quercus spp.	Angiosperm	31	0.021	0.027743	Kahl et al. 2017
Quercus spp.	Angiosperm	43	0.0175	0.014815	MacMillan 1988
Quercus spp.	Angiosperm	30	0.28	0.254599	Schowalter 1992
Quercus spp.	Angiosperm	30	0.069	0.069421	Schowalter 1998
Sequoia sempervirens	Gymnosperm	10	0.024	0.01738	T. Busing and Fijumori 2005
Sequoiadendron giganteum	Gymnosperm	litter	0.07	0.089325	Stohlgren 1988

full_name	classification	size_class_cm	k_const	climate_normalized_k	ref
Thuja plicata	Gymnosperm	52	0.007	0.007	Harmon 2005
Thuja plicata	Gymnosperm	logs	0.009	0.011683	Sollins et al. 1987
Tsuga canadensis	Gymnosperm	10	0.04	0.040799	Harmon 1982
Tsuga canadensis	Gymnosperm	7.6	0.024	0.0188	Mattson 1987
Tsuga canadensis	Gymnosperm	30	0.021	0.033781	Tyrrell and Crow 1994
Tsuga heterophylla	Gymnosperm	10	0.024	0.024	Erickson et al. 1985
Tsuga heterophylla	Gymnosperm	10	0.036	0.036	Erickson et al. 1985
Tsuga heterophylla	Gymnosperm	1.5	0.01	0.01	Erickson et al. 1985
Tsuga heterophylla	Gymnosperm	1.5	0.01	0.01	Erickson et al. 1985
Tsuga heterophylla	Gymnosperm	>30	0.0079	0.008732	Graham and Cromack 1982
Tsuga heterophylla	Gymnosperm	<30	0.023	0.025422	Graham and Cromack 1982
Tsuga heterophylla	Gymnosperm	all	0.01	0.011053	Graham and Cromack 1982
Tsuga heterophylla	Gymnosperm	52	0.023	0.023	Harmon 2005
Tsuga heterophylla	Gymnosperm	52	0.026	0.026	Harmon 2005
Tsuga heterophylla	Gymnosperm	52	0.018	0.020516	Harmon 2005
Tsuga heterophylla	Gymnosperm	log	0.015	0.017097	Janish 2005
Tsuga heterophylla	Gymnosperm	logs	0.016	0.020769	Sollins et al. 1987

APPENDIX B

Appendix B: Mean species decay values and derived decay values

Genus	**Species**	**Classification**	**k.foliage**	**Genus.mean**	**CWD**	**FWD**	**der.FWD**	**der.CWD**
Abies	amabilis	Gymnosperm	0.17356	0.044373	0.023	0.0025	0.068152	0.029374
Abies	balsamea	Gymnosperm	0.17356	0.044373	0.03145	0.078744	0.078744	NA
Abies	concolor	Gymnosperm	0.17356	0.044373	0.045	0.103	0.095729	0.050801
Abies	grandis	Gymnosperm	0.17356	0.044373	0.038	0.059	0.086954	0.015699
Abies	lasiocarpa	Gymnosperm	0.17356	0.044373	0.035	0.05086	0.083194	0.009205
Abies	magnifica	Gymnosperm	0.17356	0.044373	0.043	0.093222	0.093222	NA
Abies	procera	Gymnosperm	0.17356	0.044373	0.03	0.076926	0.076926	NA
Abies	spp.	Gymnosperm	0.17356	0.044373	0.052	0.104503	0.104503	NA
Acer	rubrum	Angiosperm	0.474167	0.0648	0.0805	0.140228	0.140228	NA
Acer	spp.	Angiosperm	0.474167	0.0648	0.0491	0.100868	0.100868	NA
Allocasuarina	fraseriana	Angiosperm	0.474167	0.082187	0.037946	0.136615	0.086886	0.077618
Alnus	rubra	Angiosperm	0.474167	0.104714	0.07	0.13075	0.127066	0.072939
Banksia	grandis	Angiosperm	0.474167	0.151818	0.070095	0.252359	0.127185	0.169953
Betula	costata	Angiosperm	0.474167	0.068375	0.03	0.076926	0.076926	NA
Betula	lenta	Angiosperm	0.474167	0.068375	0.149	0.226094	0.226094	NA
Betula	papyrifera	Angiosperm	0.474167	0.068375	0.053	0.105757	0.105757	NA
Betula	pendula	Angiosperm	0.474167	0.068375	0.0562	0.139	0.109768	0.07952
Betula	spp.	Angiosperm	0.474167	0.068375	0.056	0.109517	0.109517	NA
Calocedrus	decurrens	Gymnosperm	0.17356	0.09	0.02	0.16	0.064391	0.096273
Carpinus	spp.	Angiosperm	0.474167	0.083	0.083	0.143362	0.143362	NA
Carya	spp.	Angiosperm	0.474167	0.093667	0.093667	0.156733	0.156733	NA

Genus	Species	Classification	k.foliage	Genus.mean	CWD	FWD	der.FWD	der.CWD
Castanea	dentata	Angiosperm	0.474167	0.041	0.00134	0.041	NA	0.00134
Cornus	florida	Angiosperm	0.474167	0.0875	0.05	0.125	0.101996	0.068351
Cornus/Quercus	spp.	Angiosperm	0.474167	0.080333	0.032718	0.080333	NA	0.032718
Corylus	avellana	Angiosperm	0.474167	0.189	0.119408	0.189	NA	0.119408
Diospyros	virginiana	Angiosperm	0.474167	0.261	0.261	0.366487	0.366487	NA
Eucalyptus	calophylla	Angiosperm	0.474167	0.121797	0.113311	0.407949	0.181357	0.294077
Eucalyptus	diversicolor	Angiosperm	0.474167	0.121797	0.056851	0.121192	0.110585	0.065314
Eucalyptus	maculata	Angiosperm	0.474167	0.121797	0.049	0.100743	0.100743	NA
Eucalyptus	marginata	Angiosperm	0.474167	0.121797	0.035311	0.127128	0.083583	0.070049
Eucalyptus	spp.	Angiosperm	0.474167	0.121797	0.059095	0.169545	NA	NA
Eucalyptus	regnans	Angiosperm	0.474167	0.121797	0.041	0.090715	0.090715	NA
Fagus	spp.	Angiosperm	0.474167	0.149725	0.04395	0.094413	0.094413	NA
Fagus	sylvatica	Angiosperm	0.474167	0.149725	0.172459	0.2555	NA	0.172459
Fraxinus	excelsior	Angiosperm	0.474167	0.069	0.042025	0.092	NA	0.042025
Fraxinus	profunda	Angiosperm	0.474167	0.069	0.071	0.071	0.12832	0.025272
Fraxinus	spp.	Angiosperm	0.474167	0.069	0.019	0.063138	0.063138	NA
Juniperus	communis	Gymnosperm	0.17356	0.0365	0.00225	0.0365	NA	0.00225
Kalmia	latifolia	Angiosperm	0.474167	0.037	0.037	0.085701	0.085701	NA
Larix	dahurica	Gymnosperm	0.17356	0.01825	0.015	0.058123	0.058123	NA
Larix	siberica	Gymnosperm	0.17356	0.01825	0.027	0.073166	0.073166	NA
Larix	spp.	Gymnosperm	0.17356	0.01825	0.004	0.044335	0.044335	NA
Liriodendron	tulipifera	Angiosperm	0.474167	0.107	0.053992	0.107	NA	0.053992
Mixed		Angiosperm	0.474167	0.01177	0.01177	0.054075	0.054075	NA
Nyssa	sylvatica	Angiosperm	0.474167	0.163	0.163	0.243643	0.243643	NA
Oxydendrum	arboreum	Angiosperm	0.474167	0.0415	0.0415	0.091341	0.091341	NA
Picea	abies	Gymnosperm	0.17356	0.027449	0.0355	0.0275	0.08382	0.00943

Genus	Species	Classification	k.foliage	Genus.mean	CWD	FWD	der.FWD	der.CWD
Picea	ajanensis	Gymnosperm	0.17356	0.027449	0.028	0.074419	0.074419	NA
Picea	engelmannii	Gymnosperm	0.17356	0.027449	0.00774	0.0407	0.049023	0.0011
Picea	glauca	Gymnosperm	0.17356	0.027449	0.0545	0.107637	0.107637	NA
Picea	obovata	Gymnosperm	0.17356	0.027449	0.049	0.100743	0.100743	NA
Picea	rubens	Gymnosperm	0.17356	0.027449	0.030667	0.077762	0.077762	NA
Picea	sitchensis	Gymnosperm	0.17356	0.027449	0.0139	0.056745	0.056745	NA
Picea	spp.	Gymnosperm	0.17356	0.027449	0.0345	0.082567	0.082567	NA
Pinus	albicaulis	Gymnosperm	0.17356	0.043368	0.022347	0.067333	NA	0.022347
Pinus	banksiana	Gymnosperm	0.17356	0.043368	0.031	0.07818	0.07818	NA
Pinus	contorta	Gymnosperm	0.17356	0.043368	0.019844	0.0572	0.064196	0.014263
Pinus	jefferyi	Gymnosperm	0.17356	0.043368	0.042	0.091968	0.091968	NA
Pinus	koraiensis	Gymnosperm	0.17356	0.043368	0.015	0.058123	0.058123	NA
Pinus	lambertiana	Gymnosperm	0.17356	0.043368	0.036	0.11	0.084447	0.056385
Pinus	monticola	Gymnosperm	0.17356	0.043368	0.035	0.083194	0.083194	NA
Pinus	pinaster	Gymnosperm	0.17356	0.043368	0.025824	0.092974	0.071692	0.042803
Pinus	ponderosa	Gymnosperm	0.17356	0.043368	0.015083	0.0312	0.058228	0.006478
Pinus	radiata	Gymnosperm	0.17356	0.043368	0.127	0.198517	0.198517	NA
Pinus	resinosa	Gymnosperm	0.17356	0.043368	0.055	0.108264	0.108264	NA
Pinus	rigida	Gymnosperm	0.17356	0.043368	0.06	0.063	0.114531	0.01889
Pinus	siberica	Gymnosperm	0.17356	0.043368	0.019	0.063138	0.063138	NA
Pinus	sibirica	Gymnosperm	0.17356	0.043368	0.014	0.05687	0.05687	NA
Pinus	spp.	Gymnosperm	0.17356	0.043368	0.0245	0.070032	0.070032	NA
Pinus	sylvestris	Gymnosperm	0.17356	0.043368	0.030813	0.079	0.077945	0.031654
Pinus	taeda	Gymnosperm	0.17356	0.043368	0.0565	0.058	0.110144	0.014901
Pinus	virginiana	Gymnosperm	0.17356	0.043368	0.04	0.089461	0.089461	NA
Populus	spp.	Angiosperm	0.474167	0.054667	0.055	0.108264	0.108264	NA

Genus	Species	Classification	k.foliage	Genus.mean	CWD	FWD	der.FWD	der.CWD
Populus	tremula	Angiosperm	0.474167	0.054667	0.0575	0.111398	0.111398	NA
Populus	tremuloides	Angiosperm	0.474167	0.054667	0.07	0.127066	0.127066	NA
Prunus	spp.	Angiosperm	0.474167	0.031	0.031	0.07818	0.07818	NA
Psuedotsuga	menziesii	Gymnosperm	0.17356	0.027103	0.021072	0.037385	0.065735	0.001545
Psuedotsuga	spp.	Gymnosperm	0.17356	0.027103	0.002	0.041828	0.041828	NA
Quercus	alba	Angiosperm	0.474167	0.142455	0.063	0.118292	0.118292	NA
Quercus	coccinea	Angiosperm	0.474167	0.142455	0.075	0.133334	0.133334	NA
Quercus	prinus	Angiosperm	0.474167	0.142455	0.175	0.1122	0.258685	0.05814
Quercus	robur	Angiosperm	0.474167	0.142455	0.124394	0.19525	NA	0.124394
Quercus	spp.	Angiosperm	0.474167	0.142455	0.096875	0.160755	0.160755	NA
Rhododendron	maximum	Angiosperm	0.474167	0.059	0.015699	0.059	NA	0.015699
Robinia	pseudoacacia	Angiosperm	0.474167	0.015	0.015	0.058123	0.058123	NA
Sequoia	sempervirens	Gymnosperm	0.17356	0.024	0.012222	0.024	NA	0.012222
Sequoiadendron	giganteum	Gymnosperm	0.17356	0.07	0.024475	0.07	NA	0.024475
Thuja	plicata	Gymnosperm	0.17356	0.0358	0.008	0.054333	0.049349	0.011976
Tilia	spp.	Angiosperm	0.474167	0.035	0.035	0.083194	0.083194	NA
Tsuga	canadensis	Gymnosperm	0.17356	0.019731	0.0305	0.024	0.077553	0.012222
Tsuga	heterophylla	Gymnosperm	0.17356	0.019731	0.019155	0.01	0.063331	0.023391
Other hardwood	Spp.	Angiosperm	0.474167	0.095868	0.064499	0.159492	NA	NA
Other softwood	Spp.	Gymnosperm	0.17356	0.035882	0.004513	0.084299	NA	NA

APPENDIX C

Appendix C: 95th percentile climate modifier values

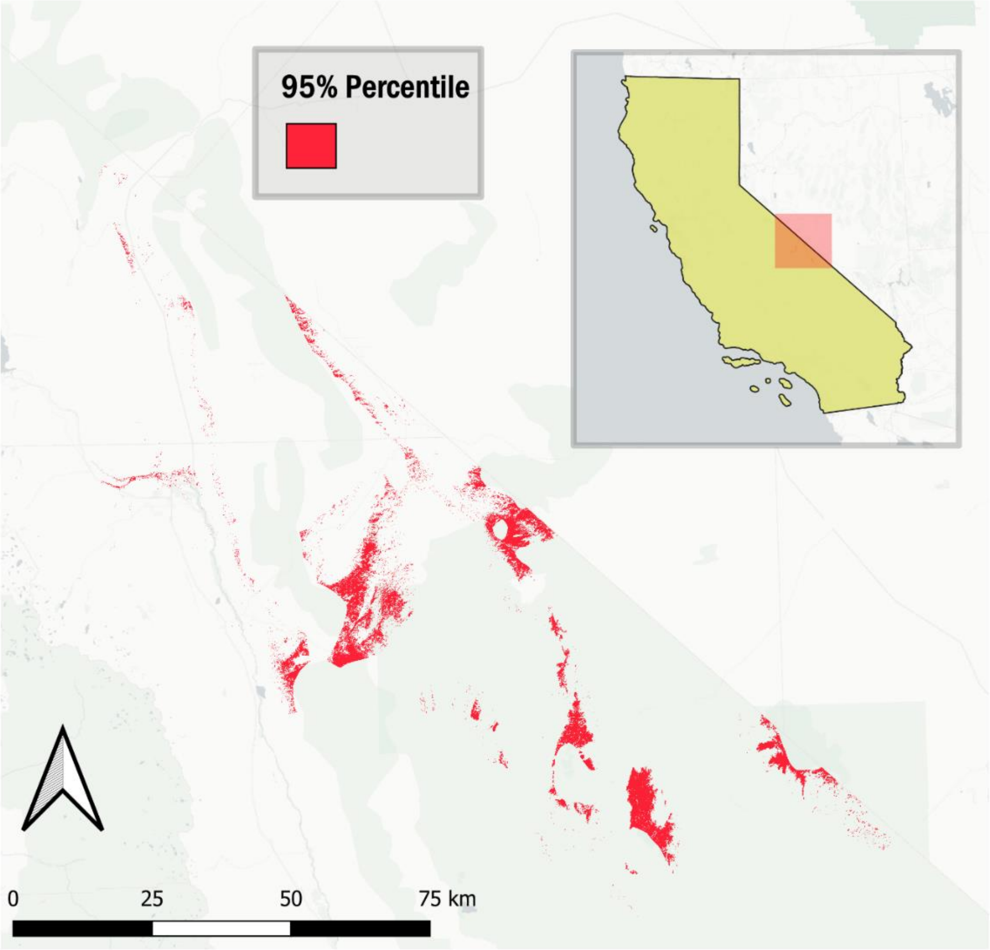

Figure 14: Area of climate modifier values which fall within the 95% percentile range. These are the extreme high values of the climate modifier that appear in the Eastern Sierras and Nevada border.